

---

# NON-PARAMETRIC ESTIMATION OF TRANSITION INTENSITIES IN INTERVAL CENSORED MARKOV MULTI-STATE MODELS WITHOUT LOOPS

---

Daniel Gomon <sup>1,\*</sup>, Hein Putter <sup>1,2</sup>

<sup>1</sup> *Mathematical Institute, Leiden University, Einsteinweg 55, Leiden, the Netherlands*

<sup>2</sup> *Department of Biomedical Data Sciences, Leiden University Medical Centre, Einthovenweg 20, Leiden, the Netherlands*

## ABSTRACT

Panel data arises when transitions between different states are interval-censored in multi-state data. The analysis of such data using non-parametric multi-state models was not possible until recently, but is very desirable as it allows for more flexibility than its parametric counterparts. The single available result to date has some unique drawbacks. We propose a non-parametric estimator of the transition intensities for panel data using an Expectation Maximisation algorithm. The method allows for a mix of interval-censored and right-censored (exactly observed) transitions. A condition to check for the convergence of the algorithm to the non-parametric maximum likelihood estimator is given. A simulation study comparing the proposed estimator to a consistent estimator is performed, and shown to yield near identical estimates at smaller computational cost. A data set on the emergence of teeth in children is analysed. Code to perform the analyses is publicly available.

**Keywords** Multi-state model · Markov · NPMLE · EM algorithm · interval censoring · panel data

## 1 Introduction

Non-parametric estimators such as the Kaplan-Meier survival curve are very popular in the standard survival setting with right-censored time to event data. Their popularity comes from their flexibility, as they do not require assumptions to be made on the underlying form of the hazard rate. Research in survival analysis is very focused on right-censored data, where event times are either observed exactly or known to occur after a certain censoring time. Many real life scenarios however generate interval-censored data, where event times are only known to lie between two observation times. Such data often arises in medical studies, where patients are observed periodically over an extended interval of time. Non-parametric estimators have also been derived for interval-censored data. Examples and an overview of analysis techniques for interval-censored data are given in Bogaerts et al. (2020) [1]. An important quantity in this setting is Turnbull's non-parametric estimator for the survival function [2]. Due to the additional complexity of interval-censored data, the estimator requires the use of an Expectation Maximization (EM) algorithm. It might therefore be desirable to negate the need to use interval-censored techniques, for example by using imputation techniques to recover the "missing" event time or ignore the missingness mechanism altogether and using techniques for right-censored data instead. These approaches can lead to biases and incorrect inference [3, 4]. It is therefore important to use appropriate techniques in the presence of interval-censored data.

The standard survival setting with a single time-to-event outcome is often insufficient to describe the data-generating mechanism of a study. As an example, illness often precedes death in medical studies and the interest may lie in modelling both the time to death and time to illness. This situation can be well described using an (extended) illness-death model (Figure 1a), where a subject can make transitions between the three states. These models are examples of a multi-state model, a powerful generalisation of the standard survival setting where the data is described using states (such as illness, death) and transitions (becoming ill, dying when healthy). Under the Markov assumption, the cumulative intensities can be non-parametrically estimated for multi-state models with right-censored data using the Nelson-Aalen estimator and translated into transition probabilities using the Aalen-Johanssen estimator [5]. Theory and practical applications are well described in many textbooks and tutorials [6, 7, 8].

---

\*Corresponding Author, d.gomon@math.leidenuniv.nl

Interval-censored data also arise in a multi-state setting, when the state a subject resides in is observed periodically. As a result so called *panel data* are collected, where transitions between states are interval-censored. Although non-parametric estimation in multi-state models has been well studied in the right-censored setting, until recently results for general interval-censored multi-state models were mostly lacking (Chapter 5 of Cook & Lawless [6]). Existing models either assume (piecewise-)constant intensity functions [9, 10] or are restricted to specific multi-state models [11, 12] and smoothness assumptions [13, 14]. A non-parametric estimator for general interval-censored multi-state models was recently derived by Gu et al. [15, 16] using an EM algorithm with latent Poisson variables. The use of latent Poisson variables introduces some challenges, which we circumvent by taking a different approach.

In this article, we propose an Expectation Maximization algorithm to non-parametrically estimate the transition intensities in a Markov multi-state model without loops. We extend the algorithm to allow for transitions to an arbitrary but fixed number of states to be observed at exact times, facilitating the analysis of a mix of interval- and right-censored data. The notation, theory and EM algorithm are described in Section 2. In Section 2.5, the EM algorithm is described in detail and a method to determine convergence of the algorithm is given, similarly to [17]. The latent Poisson estimator [15] is described in Section 2.6 and used for comparison throughout the rest of the article. A simulation study is performed in Section 3, where the proposed estimator is compared with the latent Poisson [15] and the time-homogeneous [9] approach. The three aforementioned methods are then used to analyse the Signal-Tandmobiël study [18] on tooth emergence in children. The article is concluded by a discussion and recommendations for future research.

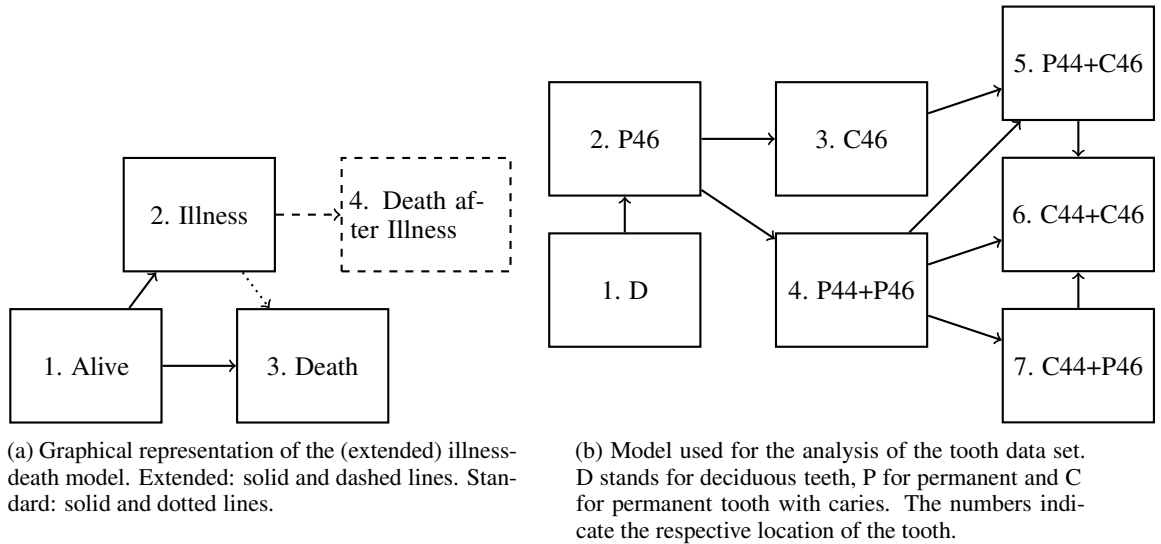


Figure 1: Graphical display of two multi-state models.

## 2 Methods

In this section notation for multi-state models and data is introduced, as well as the proposed estimator. For further details on multi-state modelling, the reader is referred to [6, 7].

### 2.1 Theory

Let  $X(t)$  represent a time non-homogeneous Markov multi-state model with states in  $\mathcal{H} = \{1, \dots, H\}$  and denote the history (filtration) of the process up until time  $t$  as  $\mathcal{F}_t = \{X(u); 0 \leq u \leq t\}$ . Not all transitions between states in  $\mathcal{H}$  will be possible, we therefore let  $\mathcal{V} = \{(g, h) \in \mathcal{H} \times \mathcal{H}; \text{direct transition } g \rightarrow h \text{ is possible}\}$  denote the set of possible direct transitions. For  $(g, h) \in \mathcal{V}$  let the counting process  $N_{gh}(t)$  denote the number of  $g \rightarrow h$  transitions in  $[0, t]$  and  $dN_{gh}(t) = \lim_{dt \downarrow 0} N_{gh}(t) - N_{gh}(t - dt)$ . As the counting processes for all transitions contain complete information on the process history, it can also be represented as  $\mathcal{F}_t = \{N_{gh}(u); (g, h) \in \mathcal{V}, 0 \leq u \leq t\}$ .

The transition intensity, describing the instantaneous risk of a transition from state  $g$  to  $h$  with  $g, h \in \mathcal{H}$  is given by:

$$\alpha_{gh}(t) = \lim_{dt \downarrow 0} \frac{\mathbb{P}(X(t+dt) = h | X(t) = g, \mathcal{F}_{t-})}{dt} = \lim_{dt \downarrow 0} \frac{\mathbb{P}(X(t+dt) = h | X(t) = g)}{dt},$$

where the second equality holds due to the Markov assumption. The cumulative transition intensity is then simply the integral  $A_{gh}(t) = \int_0^t \alpha_{gh}(s) ds$ . The process is only at risk of a transition at times when said transition can occur, therefore we also consider the transition intensity process:

$$\lambda_{gh}(s) = \alpha_{gh}(s) Y_g(s),$$

with  $Y_g(s) = \mathbb{1}\{X(s-) = g\}$  the at-risk indicator for transitions out of state  $g$ . The intensity process is zero whenever the process is not at risk of a transition. Let  $C$  denote a right-censoring time after which the state of the process is no longer known.

Determining the probability of transitioning to one state from another is a vital component of multi-state modelling. This quantity is given by the transition probabilities:

$$P_{gh}(s, t) = \mathbb{P}(X(t) = h | X(s) = g).$$

We gather the cumulative intensities and transition probabilities into  $H \times H$  matrices  $\mathbf{A}(t) = \{A_{gh}(t); g, h \in \mathcal{H}\}$  with diagonal entries  $A_{gg}(t) = -\sum_{h \neq g} A_{gh}(t)$  and  $\mathbf{P}(s, t) = \{P_{gh}(s, t); g, h \in \mathcal{H}\}$  for  $s, t \geq 0$ . For Markov multi-state models, the Chapman-Kolmogorov equations allow us to relate the transition probabilities to the transition intensities through product integration:

$$\mathbf{P}(s, t) = \prod_{s < u \leq t} (\mathbf{I} + d\mathbf{A}(u)). \quad (1)$$

## 2.2 Data

We consider panel data, where subjects  $i = 1, \dots, n$  are observed to be in state  $x_{ij} \in \mathcal{H}$  at random (or possibly fixed) subject-specific visit times  $T_{ij}$  with  $j = 1, \dots, n_i$ . We denote  $t_{ij}$  for the observed values of  $T_{ij}$ . Following Section 5.5 of [6] we assume that the subject observation times follow a conditionally independent visit process:

$$T_{ij} \perp \{X_i(s), s > t_{i,j-1}\} | \mathcal{F}_{t_{i,j-1}}.$$

This means that the next visit time must not depend on the state of the process since the last visit time, but can depend on all information available at the last visit time. Additionally, we make the assumption of independent censoring:

$$\alpha_{gh}(t) = \lim_{dt \downarrow 0} \frac{\mathbb{P}(X(t+dt) = h | X(t) = g, C > t)}{dt}.$$

In other words, the knowledge that the process is currently uncensored does not influence the intensities.

The observed set of information for subject  $i$  is then given by:

$$\mathbb{X}_i^O = \{(x_{i0}, t_{i0}), (x_{i1}, t_{i1}), \dots, (x_{in_i}, t_{in_i})\}. \quad (2)$$

For each subject we therefore observe realisations  $X_i(t)$  of  $X(t)$  such that  $X_i(t_{ij}) = x_{ij}$ . The observed data likelihood for panel data is then given by:

$$L^O = \prod_{i=1}^n \prod_{j=1}^{n_i} P_{x_{i,j-1} x_{ij}}(t_{ij-1}, t_{ij}). \quad (3)$$

Let  $0 = \tau_0 < \tau_1 < \dots < \tau_K < \infty$  be the sorted unique time points of the set  $\{t_{ij}; i = 1, \dots, n, j = 1, \dots, n_i\}$ , and let  $\mathcal{T} = \{\tau_k; k = 1, \dots, K\}$ . We shall refer to an interval  $(\tau_{k-1}, \tau_k]$  for an arbitrary  $k$  as a **bin**. Define for each subject  $i$  and state  $g$  the at risk indicator  $Y_{g,i}(s) = \mathbb{1}\{X_i(s-) = g\}$ , indicating whether subject  $i$  is in state  $g$  just before time  $s$  and let  $N_{gh,i}(t)$  count the number of transitions  $g \rightarrow h$  of subject  $i$  in  $[0, t]$ . Note that the true state is only known at the observation times of the subjects. The value of  $Y_{g,i}(s)$  is therefore only known right after the observation times. The number of transitions may be known if only a single path could have been taken by subject  $i$ , but this is not often the case. Similarly, we define  $\lambda_{gh,i}(t) = \alpha_{gh}(t) Y_{g,i}(t)$  and  $dN_{gh,i}(t) = \lim_{dt \downarrow 0} N_{gh,i}(t) - N_{gh,i}(t - dt)$ . For fixed  $k \in \{1, \dots, K\}$  we define:

$$l_i^k = \max_{j=1, \dots, n_i} \{t_{ij}; t_{ij} \leq \tau_{k-1}\}, r_i^k = \min_{j=1, \dots, n_i} \{t_{ij}; t_{ij} \geq \tau_k\},$$

so that  $(l_i^k, r_i^k]$  is the observational interval of subject  $i$  containing  $(\tau_{k-1}, \tau_k]$ . Additionally, let  $a_i^k = X_i(l_i^k)$  and  $b_i^k = X_i(r_i^k)$  be the corresponding states occupied at the ends of this observational interval. We define  $B_i^k := \{X_i(t_{ij}), t_{ij} \leq l_i^k\}$  and  $F_i^k := \{X_i(t_{ij}), t_{ij} \geq r_i^k\}$  as the past and future observations relative to the interval  $[l_i^k, r_i^k]$ . A graphical representation of this notation can be found in Supplementary Materials section A.

## 2.3 Model - Panel data

In this section we will non-parametrically estimate the transition intensities  $\alpha_{gh}(t)$  for panel data using the Expectation Maximisation (EM) algorithm [19]. The EM algorithm is an iterative procedure used to find maximum likelihood estimates in the presence of missing data. In the case of panel data, the exact transition times between states are missing for individuals, warranting the use of this algorithm.

### 2.3.1 Complete-data likelihood

To employ the EM algorithm, we must first determine the complete data likelihood. Suppose we observe all transitions for all subjects and therefore know the exact transition times  $a_{ij}$  for  $j = 1, \dots, f_i$ . For each subject  $i$  we then have the following set of observations:

$$\mathbb{X}_i^C = \{(s_{i0}, a_{i0}), (s_{i1}, a_{i1}), \dots, (s_{if_i}, a_{if_i})\},$$

with  $X_i(a_{ij}) = s_{ij}$ . Under the assumption of independent censoring, the complete data likelihood contribution for a single subject is given by ([7]):

$$L_i^C = \prod_{t \leq a_{if_i}} \left\{ \prod_{(g,h) \in \mathcal{V}} (\lambda_{gh,i}(t) dt)^{dN_{gh,i}(t)} \right\} \exp \left( - \sum_{(g,h) \in \mathcal{V}} \int_0^{a_{if_i}} \lambda_{gh,i}(u) du \right). \quad (4)$$

The log likelihood contribution for a single subject is then:

$$\ell_i^C := \log(L_i^C) = \int_0^{a_{if_i}} \sum_{(g,h) \in \mathcal{V}} \left\{ \log(\alpha_{gh}(t) Y_{g,i}(t)) dN_{gh,i}(t) - \alpha_{gh}(u) Y_{g,i}(u) du \right\}.$$

Let us define  $\alpha_{gh}^k := \int_{\tau_{k-1}}^{\tau_k} \alpha_{gh}(t) dt$ ,  $Y_{g,i}^k := \int_{\tau_{k-1}}^{\tau_k} Y_{g,i}(t) dt$  and  $d_{gh,i}^k := \int_{\tau_{k-1}}^{\tau_k} dN_{gh,i}(t)$ . These quantities then represent the cumulative intensity, time spent in  $g$  and transitions made between  $g$  and  $h$  respectively, in the  $k$ -th bin. The NPMLE of the cumulative intensity for interval-censored data in the standard survival setting (two state model with alive and dead) has been shown to only have jumps at some of the unique observation times [2]. Later, a similar result was found for the progressive three state model [11] and the illness-death model [12]. The general result is that the jumps in the cumulative intensities are completely determined by the right-endpoints of the support intervals (the intervals where the intensities are non-zero). The support intervals in turn depend solely on the unique observation times. We do not know in advance what the support intervals are for general multi-state models, therefore we assume the cumulative intensities can only make jumps at any of the unique observation times  $\mathcal{T}$ . Asymptotically, note that as  $n \rightarrow \infty$  we will have that  $\max_k |\tau_k - \tau_{k-1}| \rightarrow 0$ . In this limit and under above assumption,  $A_{gh}(t)$  will start to resemble a smooth function similar to the Nelson-Aalen estimator [20, 21]. We then have that  $\alpha_{gh}^k = \alpha_{gh}(\tau_k)$ ,  $Y_{g,i}^k = Y_{g,i}(\tau_k)$  and  $d_{gh,i}^k = dN_{gh,i}(\tau_k)$  for  $k = 1, \dots, K$ . Above integrals then reduce to sums:

$$\ell_i^C = \sum_{k=1}^K \sum_{(g,h) \in \mathcal{V}} \left\{ \log(\alpha_{gh}^k Y_{g,i}^k) d_{gh,i}^k - \alpha_{gh}^k Y_{g,i}^k \right\} = \sum_{k=1}^K \sum_{(g,h) \in \mathcal{V}} \left\{ \log(\alpha_{gh}^k) d_{gh,i}^k - \alpha_{gh}^k Y_{g,i}^k \right\}.$$

The second equality holds because  $d_{gh,i}^k = 1$  implies  $Y_{g,i}^k = 1$ , and  $d_{gh,i}^k = 1$  is only possible if  $Y_{g,i}^k = 1$ . Now the complete-data log likelihood is obtained by summing over all subjects:

$$\ell^C = \sum_{i=1}^n \ell_i^C = \sum_{k=1}^K \sum_{(g,h) \in \mathcal{V}} \left\{ d_{gh}^k \log(\alpha_{gh}^k) - \alpha_{gh}^k Y_g^k \right\}, \quad (5)$$

with  $d_{gh}^k := \sum_{i=1}^n d_{gh,i}^k$  and  $Y_g^k := \sum_{i=1}^n Y_{g,i}^k$ .

### 2.3.2 E-step

In the E-step of the EM algorithm we calculate the expected value of the complete-data likelihood using an initial guess for the intensities of all transitions. We then determine new estimates for the intensities in the M-step by maximising the complete data likelihood and repeat this until convergence. Denote by  $\alpha = (\alpha_{gh}^k; g \neq h \in \mathcal{H}, k = 1, \dots, K)$  the vector of (true) intensities, and with  $\tilde{\alpha} = (\tilde{\alpha}_{gh}^k; g \neq h \in \mathcal{H}, k = 1, \dots, K)$  the current estimate. Let  $O = \{\mathbb{X}_i^O; i = 1, \dots, n\}$  denote the observed data and  $C = \{\mathbb{X}_i^C; i = 1, \dots, n\}$  the complete data.

The main goal is to calculate the conditional expectation of the complete data log-likelihood function:

$$\mathbb{E}[\ell^C | O, \tilde{\alpha}] = \sum_{k=1}^K \sum_{(g,h) \in \mathcal{V}} \{ \mathbb{E} [d_{gh}^k | O, \tilde{\alpha}] \log(\alpha_{gh}^k) - \alpha_{gh}^k \mathbb{E} [Y_g^k | O, \tilde{\alpha}] \} \quad (6)$$

Note that this requires us to determine two conditional expectations. It can be shown that:

$$d_{gh}^k(\tilde{\alpha}) := \mathbb{E} [d_{gh}^k | O, \tilde{\alpha}] = \sum_{i=1}^n \frac{\tilde{P}_{\alpha_i^k, g}(l_i^k, \tau_{k-1}) \cdot \tilde{\alpha}_{gh}^k \cdot \tilde{P}_{h, b_i^k}(\tau_k, r_i^k)}{\tilde{P}_{\alpha_i^k, b_i^k}(l_i^k, r_i^k)}, \quad (7)$$

$$Y_g^k(\tilde{\alpha}) := \mathbb{E} [Y_g^k | O, \tilde{\alpha}] = \sum_{i=1}^n \frac{\tilde{P}_{\alpha_i^k, g}(l_i^k, \tau_{k-1}) \cdot \tilde{P}_{g, b_i^k}(\tau_{k-1}, r_i^k)}{\tilde{P}_{\alpha_i^k, b_i^k}(l_i^k, r_i^k)}, \quad (8)$$

with  $\tilde{\mathbf{P}}(s, t) = \prod_{s < u \leq t} (\mathbf{I} + d\tilde{\mathbf{A}}(u))$  the product integral of the current estimates of the transition intensities. The derivation can be found in the Supplementary Materials section B.

### 2.3.3 M-step

Having found the expected value of the likelihood function under the current estimates of the parameters, we need to maximise the resulting expected likelihood function. The jumps in the cumulative intensities are bounded, so the maximum must be found within a restricted optimisation space. Luckily, the complete data log-likelihood is a concave function and therefore we can use convex optimisation theory [22].

The intensities  $\alpha_{gh}^k$  represent conditional probabilities of making a transition in a single bin and therefore must be bounded by zero and one. Additionally, the total probability of leaving a state  $g$  in any bin  $k$  must also be smaller or equal than one. We therefore define the following optimisation region:

$$C_\alpha = \left\{ \alpha_{gh}^k, g, h \in \mathcal{H}, k = 1, \dots, K; \alpha_{gh}^k \geq 0, \sum_{h \leftarrow g} \alpha_{gh}^k \leq 1 \right\},$$

where  $\sum_{h \leftarrow g}$  represents the sum over all states  $h$  that can be reached directly (in a single transition) from  $g$ . Note that the two conditions  $\alpha_{gh}^k \geq 0$  and  $\sum_{h \leftarrow g} \alpha_{gh}^k = 1$  guarantee that  $0 \leq \alpha_{gh}^k \leq 1$ . We show in the Supplementary Materials Section B that the expected value of the complete data likelihood is maximised over the above region by the following expression:

$$\alpha_{gh}^k = \begin{cases} \frac{d_{gh}^k(\tilde{\alpha})}{Y_g^k(\tilde{\alpha})}, & \mu_g^k = 0, \\ \frac{d_{gh}^k(\tilde{\alpha})}{\sum_{h \leftarrow g} d_{gh}^k(\tilde{\alpha})}, & \mu_g^k > 0, \end{cases} \quad (9)$$

with

$$\mu_g^k = \max \left( 0, \sum_{h \leftarrow g} d_{gh}^k(\tilde{\alpha}) - Y_g^k(\tilde{\alpha}) \right). \quad (10)$$

Having found this expression, we can employ the EM algorithm until a certain convergence criterion is met, see Algorithm (1).

## 2.4 Model - Panel data with exactly observed transition times

Until now we have considered the case of interval censored panel data. In multi-state models there are often states for which the entry time into the state is exactly observed (or right-censored). In the illness-death model for example, it is unlikely that the exact time of the occurrence of a disease is known but the exact time of death is almost always known. These ‘‘exactly observed’’ states are oftentimes absorbing, but we do not have to make this assumption. In this section we therefore consider the possibility of transitions into a fixed and known subset of  $\mathcal{E} \subseteq \mathcal{H}$  to be observed at exact times, so that  $x_{ij} \in \mathcal{E}$  implies that the transition to  $x_{ij}$  happened at  $t_{ij}$ . To derive the intensities with exactly observed states, we follow the same steps as in Section 2.3.

Suppose we observe a subject in state  $h \in \mathcal{E}$  at time  $\tau_k$  for some  $k \in \{1, \dots, K\}$ . This means that the process must have been in a state  $g \in \mathcal{H}$  which allows for a direct transition to  $h$  right before time  $\tau_k$ . Define  $\mathcal{R}_h = \{g \in$

$\mathcal{H}$ ; direct transition  $g \rightarrow h$  is possible} as the states which  $h \in \mathcal{H}$  is directly reachable from. As we assumed that the cumulative intensities have upward jumps only at times in  $\mathcal{T}$ , we therefore know that the subject must have been in  $\mathcal{R}_h$  at time  $\tau_k^- = \tau_{k-1}$ . The observed data likelihood is now given by:

$$L_E^O = \prod_{i=1}^n \prod_{j=1}^n \{P_{x_{ij-1}x_{ij}}(t_{ij-1}, t_{ij})\}^{1-\mathbb{1}\{x_{ij} \in \mathcal{E}\}} \left\{ \sum_{m \in \mathcal{R}_{x_{ij}}} P_{x_{ij-1}m}(t_{ij-1}, t_{ij-}) P_{mx_{ij}}(t_{ij-}, t_{ij}) \right\}^{\mathbb{1}\{x_{ij} \in \mathcal{E}\}}, \quad (11)$$

as opposed to Equation (3). On the other hand, the complete data still consists of all (exact) transition times, therefore the complete-data likelihood (Equation (5)) does not change. In the E-step however, we now have additional information for the calculation of the expected values whenever a state in  $\mathcal{E}$  is observed.

#### 2.4.1 E-step

To incorporate the newly available information, we re-evaluate the quantities  $d_{gh}^k(\tilde{\alpha})$  and  $Y_g^k(\tilde{\alpha})$ . We show in the Supplementary Materials Section B that when  $b_i^k \in \mathcal{E}$  the conditional expectations are instead given by:

$$d_{gh,i}^k(\tilde{\alpha}) := \mathbb{E} [d_{gh,i}^k | O, \tilde{\alpha}] = \frac{\tilde{P}_{a_i^k g}(l_i^k, \tau_{k-1}) \cdot \tilde{\alpha}_{gh}^k \cdot \sum_{m \in \mathcal{R}_{b_i^k}} \tilde{\alpha}_{mb_i^k}^{k_{r_i}} \tilde{P}_{hm}(\tau_k, \tau_{k_{r_i}-1})}{\sum_{m \in \mathcal{R}_{b_i^k}} \tilde{\alpha}_{mb_i^k}^{k_{r_i}} \tilde{P}_{a_i^k m}(l_i^k, \tau_{k_{r_i}-1})}, \quad (12)$$

$$Y_{g,i}^k(\tilde{\alpha}) := \mathbb{E} [Y_{g,i}^k | O, \tilde{\alpha}] = \frac{\tilde{P}_{a_i^k g}(l_i^k, \tau_{k-1}) \cdot \sum_{m \in \mathcal{R}_{b_i^k}} \tilde{\alpha}_{mb_i^k}^{k_{r_i}} \tilde{P}_{gm}(\tau_{k-1}, \tau_{k_{r_i}-1})}{\sum_{m \in \mathcal{R}_{b_i^k}} \tilde{\alpha}_{mb_i^k}^{k_{r_i}} \tilde{P}_{a_i^k m}(l_i^k, \tau_{k_{r_i}-1})}, \quad (13)$$

with  $\tau_{k_{r_i}} := \tau_i^k$ ,  $d_{gh}^k(\tilde{\alpha}) = \sum_{i=1}^n d_{gh,i}^k(\tilde{\alpha})$  and  $Y_g^k(\tilde{\alpha}) = \sum_{i=1}^n Y_{g,i}^k(\tilde{\alpha})$ . When  $b_i^k \notin \mathcal{E}$  the conditional expectations are still given by Equations (7) and (8).

#### 2.4.2 M-step

For the M-step we would like to maximise the expected complete data likelihood function. Fortunately, nothing changes with respect to Section 2.3.3, therefore we can still utilise Equation (9) to update our estimate of the intensities.

### 2.5 EM algorithm

The theory above suggests a way for the computation of the non-parametric maximum likelihood estimate of the intensities. An algorithm displaying the necessary steps to arrive at an estimate is given in Algorithm 1.

Algorithm 1 uses an intensity convergence criterion and therefore terminates after an iteration when the largest change in any intensity is smaller than the tolerance. A different criterion could also be used, such as a likelihood convergence criterion:  $|L - L_{old}| > \epsilon$ .

Having performed this procedure, we might want to determine whether the estimate has indeed converged at a maximum likelihood estimate or not. For a convex optimisation problem, whenever an estimate  $\tilde{\alpha}$  satisfies the Karush-Kuhn-Tucker conditions (details in Supplementary Materials section B we are guaranteed to have arrived at the MLE (see Section 5.5.3 of [22]). A procedure to determine whether our current estimate is an MLE is outlined in Algorithm 2. Note that the reduced gradient can be calculated during every iteration of Algorithm 1 at little cost and it is therefore possible to terminate the algorithm once the NPMLM has been reached.

### 2.6 Latent Poisson EM

Recently an EM approach for the NPMLM using latent Poisson variables has been developed [15], allowing for the inclusion of (time-dependent) covariates and random effects through a semi-parametric proportional hazards model. For comparison purposes, we consider their model without any covariates/random effects.

The main difference between their approach and ours is the complete data likelihood employed to maximise the observed-data likelihood (Equation (3)). In Section 2.3.1 we took the multinomial likelihood approach as described in Section 2.2 of [6], whereas they take a latent Poisson approach. They also assume that the cumulative intensities only have jumps at the unique event times, but consider latent Poisson variables  $W_{gh,i}^k$  for each bin instead of  $d_{gh,i}^k$  as we do. These variables then indicate whether a certain transition in a bin could have happened (latently), and assign

---

**Algorithm 1** Calculation of NPMLE of intensities in a MSM without loops.
 

---

**Input:** Initial estimate  $\tilde{\alpha}$ , Tolerance  $\epsilon$ .**Output:** Final estimate  $\alpha$ , observed data likelihood  $L$ .**Initialize:**  $L = 0$ ,  $L_{\text{old}} = -\infty$ ,  $\alpha_{gh}^k$  randomly.**Require:**  $\tilde{\alpha}_{gh}^k > 0$  if  $(g, h) \in \mathcal{V}$ ;  $\epsilon > 0$ 

```

while  $\max_{g,h,k} |\tilde{\alpha}_{gh}^k - \alpha_{gh}^k| > \epsilon$  do
  for  $g \in \mathcal{H}$  do
    for  $h \neq g \in \mathcal{H}$  do
      for  $k \in |\mathcal{T}|$  do
        Calculate  $Y_{gh}^k(\tilde{\alpha})$  using Equations (8) or (13)
        Calculate  $d_{gh}^k(\tilde{\alpha})$  using Equations (7) or (12)
        Calculate  $\mu_g^k$  using Equation (10)
        Update  $\tilde{\alpha}_{gh}^k$  using Equations (9)
      end for
    end for
  end for
   $L_{\text{old}} \leftarrow L$ 
   $\alpha \leftarrow \tilde{\alpha}$ 
  Calculate  $L$  using Equation (3) or (11)
end while

```

---



---

**Algorithm 2** Determine if an estimate of intensities is the NPMLE.
 

---

**Input:** Output of Algorithm 1.**Output:** TRUE/FALSE**Initialize:**  $L = 0$ ,  $L_{\text{old}} = -\infty$ .

```

for  $g \in \mathcal{H}$  do
  for  $h \neq g \in \mathcal{H}$  do
    for  $k \in |\mathcal{T}|$  do
      Calculate  $Y_{gh}^k(\tilde{\alpha})$ ,  $d_{gh}^k(\tilde{\alpha})$ ,  $\mu_g^k$  (see Algorithm 1)
      Calculate the reduced gradient  $\nabla_{gh}^k = Y_g^k(\tilde{\alpha}) - \frac{d_{gh}^k(\tilde{\alpha})}{\tilde{\alpha}_{gh}^k} + \mu_g^k$ 
    end for
  end for
end for
if  $\nabla_{gh}^k > 0$  for any  $g, h, k$  then
  return FALSE
else return TRUE
end if

```

---

(non)-zero mass if so. They then show that the observed data likelihood using latent Poisson variables is the same as Equation (3), therefore the observed-data likelihood can be maximised using the Poisson full data likelihood:

$$\ell_P^C = \sum_{i=1}^n \left( \sum_{k=1}^K \sum_{(g,h) \in \mathcal{V}} \mathbf{1}\{\tau_k \leq t_{in_i}\} [W_{gh,i}^k \log(\alpha_{gh}^k) - \alpha_{gh}^k - \log(W_{gh,i}^k!)] \right) \quad (14)$$

Performing an E- and M-step as we have, it is then possible to obtain an update rule for  $\alpha$ , which is described in more detail in the Supplementary Materials Section C.

Although possible in the latent Poisson setting, exactly observed event times are not considered for an arbitrary number of states [16] referring to the inconsistency problems in mixed samples NPMLE estimation [23]. Instead, they consider only the situation with a single absorbing state, for which observation times are known exactly and model the transition intensities into this state using B-splines. Due to the restriction to a single exactly observed state, we do not compare our model with the latent Poisson approach in the case of exactly observed states.

### 3 Simulation study

To investigate the performance of our proposed estimator we conduct a simulation study. Seeing as the latent Poisson EM estimator (Section 2.6) has been shown to be consistent [15], we focus on comparing our method to this estimator. Quantities of primary interest are the bias and variance of the estimator with respect to the cumulative intensities and the transition probabilities as well as computation speed.

#### 3.1 Data generation

We consider four different scenarios in this simulation study. We first cover the parameters which are equal over all scenarios. We assume that all  $n$  subjects are observed at the beginning of the study (time 0) and that all observations are censored at the end of the study after 15 years. We consider  $n = 100, 300$  and  $500$  subjects to assess the behaviour of the estimator with increasing samples. After study entry, subjects' 5 following inter-arrival times are uniformly  $[0, 4.4]$  distributed so that the mean final observation time is at 11 years and for around 8 percent of the subjects the final observation is censored. For each scenario and each number of subjects  $n$  we create  $N = 1000$  simulated data-sets.

The following simulation parameters are scenario specific. We consider the illness-death (ID) model, or the extended illness-death (EID) model (see Figure 1a). Observed states are simulated assuming underlying Weibull( $\lambda, k$ ) or Exponential( $\lambda$ ) transition intensities, with Weibull probability density function  $f(x; \lambda, k) = \lambda k x^{k-1} e^{-\lambda x^k}$ . Parameters were chosen so that the mean transition times were equal over all scenarios for comparable transitions. Subjects are either initially observed in the first (Alive) state or have an equal probability to start in the first or second (Illness) state. Finally, some states can be exactly observed. Details can be found in Table 1.

Scenario	Model	Starting states	Exact states $\mathcal{E}$	Transition intensities		
				1 $\rightarrow$ 2	1 $\rightarrow$ 3	2 $\rightarrow$ 3 $\vee$ 2 $\rightarrow$ 4
1	ID	1	$\emptyset$	Exp(0.1)	Exp(0.05)	Exp(0.1)
2	ID	{1, 2}	$\emptyset$	Exp(0.1)	Exp(0.05)	Exp(0.1)
3	ID	1	$\emptyset$	Weib(0.5, $\frac{1}{\sqrt{5}}$ )	Weib(0.5, $\frac{1}{\sqrt{10}}$ )	Weib(2, $(\frac{\Gamma(1.5)}{10})^2$ )
4	EID	1	{3, 4}	Exp(0.1)	Exp(0.05)	Exp(0.1)

Table 1: Simulation parameters for the 4 considered scenarios.

For each of the scenarios and  $n \in \{100, 300, 500\}$ , we fit three multi-state models to each of the  $N = 1000$  simulated data sets. The three considered models are the multinomial and latent Poisson EM approaches as well as the time-homogeneous approach [9] using the R [24] package `msm`. The time-homogeneous approach assumes that transition intensities are constant over time per transition, which comes down to assuming exponential transition hazards. For scenarios 1, 2 and 4 transition times are therefore generated under the time-homogeneous assumption. The initial estimates for the EM algorithms are chosen as  $\tilde{\alpha}_{gh}^k = \frac{1}{K}$  if  $(g, h) \in \mathcal{V}$  and zero elsewhere and the algorithms are terminated when the change in all transition intensities is smaller than 0.001. The time-homogeneous model is run with default parameters, letting the `msm` package determine initial estimates.

To obtain performance measures we define the estimated cumulative intensities for the  $j$ -th data set as  $\hat{A}_{gh}^j(t)$  for all  $(g, h) \in \mathcal{V}$  and transition probabilities  $\hat{P}_{gh}^j(t)$  for any tuple  $(g, h)$ . The true (oracle) values are denoted by  $A_{gh}(t)$  and  $P_{gh}(t)$ . We then calculate the bias, variance and Root Mean Squared Error (RMSE) of the estimators over an equidistantly spaced partition of  $[0, 15]$ . For the cumulative intensities, fixing  $(g, h) \in \mathcal{V}$  and  $t \in \{0, 0.1, 0.2, \dots, 15\}$  we calculate:

$$\text{Bias}(t) = \frac{\sum_{j=1}^N (\hat{A}_{gh}^j(t) - A_{gh}(t))}{N}, \quad \text{Var}(t) = \frac{1}{N-1} \sum_{j=1}^N \left( \hat{A}_{gh}^j(t) - \frac{\sum_{j=1}^N \hat{A}_{gh}^j(t)}{N} \right)^2, \quad (15)$$

and  $\text{RMSE}(t) = \sqrt{\text{Var}(t) + \text{Bias}^2(t)}$ . As we assumed the cumulative intensities to only have jumps in  $\mathcal{T}$ , we use linear interpolation to determine  $\hat{A}_{gh}^j(t)$  for  $t \notin \mathcal{T}$ . The performance measures for the transition probabilities are calculated similarly by taking the product integral (Equation (1)) over the cumulative intensities, which are interpolated first.



## 3.2 Results

For clarity we show only the results for  $n = 500$ , but the rest of the findings can be found in the Supplementary Materials Section E.

### 3.2.1 Scenario 1

In the first scenario, we consider the simple illness-death model with exponential transition hazards and all subjects starting in the alive state. Performance measures for the cumulative intensities of the three considered methods can be found in Figure 2 A. Note that the performance measures for the EM approaches are almost equal for the first two transitions. Overall, the time-homogeneous model performs best as it is correctly specified in this scenario. The multinomial and latent Poisson approach perform very similarly for transitions out of the alive state. For the transition to the death state, the estimated cumulative intensity is very unstable in the first two to three years of the study for both EM approaches, but much more so for the multinomial approach. After three years however, the intensities are recovered correctly as both the bias and variance curves remain flat over time. The reason for this instability is the small number of subjects at risk of transitioning out of the illness state in the early study times. The multinomial approach can then estimate a probability (transition intensity) close to one if only very few people are at risk and a subject makes a transition, explaining the jump of the bias curve to a value of around one.

On the other hand, the latent Poisson approach cannot change the estimates of its intensities for the  $2 \rightarrow 3$  transition before a subject has entered state 2 (see supplementary materials Section D). Because of this, the initial bias for the Poisson approach in this scenario seems smaller, but is actually completely determined by the initial estimates. As the initial estimates were chosen uniformly depending on the number of unique observation times, the variance also results purely from the difference in observation times between data sets. To illustrate this occurrence, we fit the Poisson EM model on the first 200 data-sets of this scenario using “unfortunate” initial estimates. These “unfortunate” initial estimates were chosen such that  $\sum_{k=1}^K \alpha_{gh}^k = 1$  and  $\sum_{k=1}^{\lfloor 0.1K \rfloor} \alpha_{gh}^k = 0.9$  for all  $(g, h) \in \mathcal{V}$ . In other words, we assigned 90 percent of the initial “mass” to the first 10 percent of the bins. A comparison of the results for uniform and “unfortunate” initial estimates can be found in Figure 3. Clearly, changing the initial estimates significantly changes the performance of the method for the  $2 \rightarrow 3$  transition, which is a very undesirable property.

Oftentimes, transition probabilities are of greater interest than cumulative intensities. As all subjects start in the (first) alive state in this scenario, we take a look at the bias, variance and RMSE when recovering the transition probabilities from the first state  $P_{1h}(t)$  for  $h \in \{1, 2, 3\}$ . The results can be found in Figure 2 B. Unsurprisingly the time-homogeneous approach performs best. The multinomial and Poisson approach do not seem to differ by much, but the bias for the  $1 \rightarrow 3$  transition is smaller in early time points for the multinomial approach, contrary to what was observed for the cumulative intensities. All in all, both the Poisson and multinomial approach lead to biased estimates of the cumulative intensities for different reasons. As the bias for the Poisson approach depends on the initial conditions, the multinomial estimator is more readily interpretable.

### 3.2.2 Scenario 2

The Poisson EM estimate has been shown to be consistent for the cumulative intensities [15], but only when all non-absorbing states have a positive probability to be the initially observed state. In scenario 2 both non-absorbing states are equally likely as starting states. We can therefore compare the performance of the multinomial estimator to a consistent estimator. Figure 2 C presents a comparison on the recovery of the underlying cumulative intensities.

There is not much difference between the Poisson and multinomial approach, and both perform well compared to the time-homogeneous approach. As the sample size  $n$  increases, the RMSE of the EM estimators decreases at the same rate and they converge to almost identical estimates (see Supplementary materials Section E). It is therefore reasonable to assume that our proposed estimator is also consistent for the cumulative intensities when the non-absorbing states are covered in the initial observation.

### 3.2.3 Scenario 3

In the previous scenarios, the data was generated under the time-homogeneous assumption. Now we take a look at how well the methods recover time varying intensities. The intensities for transitioning to illness and death were chosen to be decreasing functions of time, while the hazard from illness to death is increasing. In practice this means that subjects are more likely to become ill or pass away at the beginning of the study, and subjects that are ill for a long time are more likely to die. Performance measures for the cumulative intensities and transition probabilities for  $n = 500$  can be found in Figure 4 A-B.

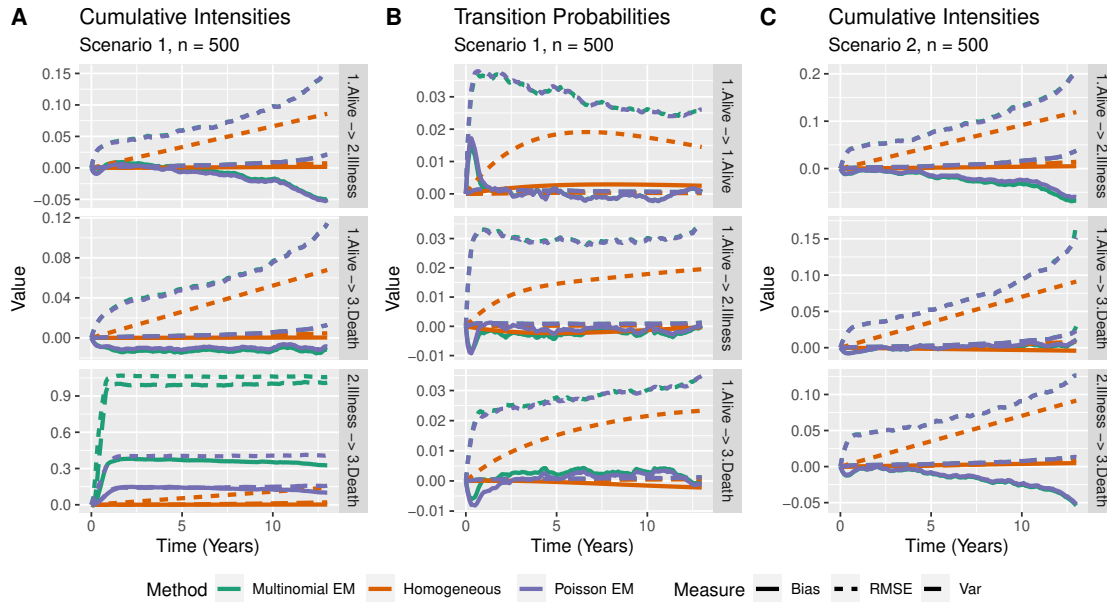


Figure 2: Bias, Variance and RMSE for  $n = 500$  subjects of A) cumulative intensities in scenario 1, B) transition probabilities in scenario 1 and C) cumulative intensities in scenario 2.

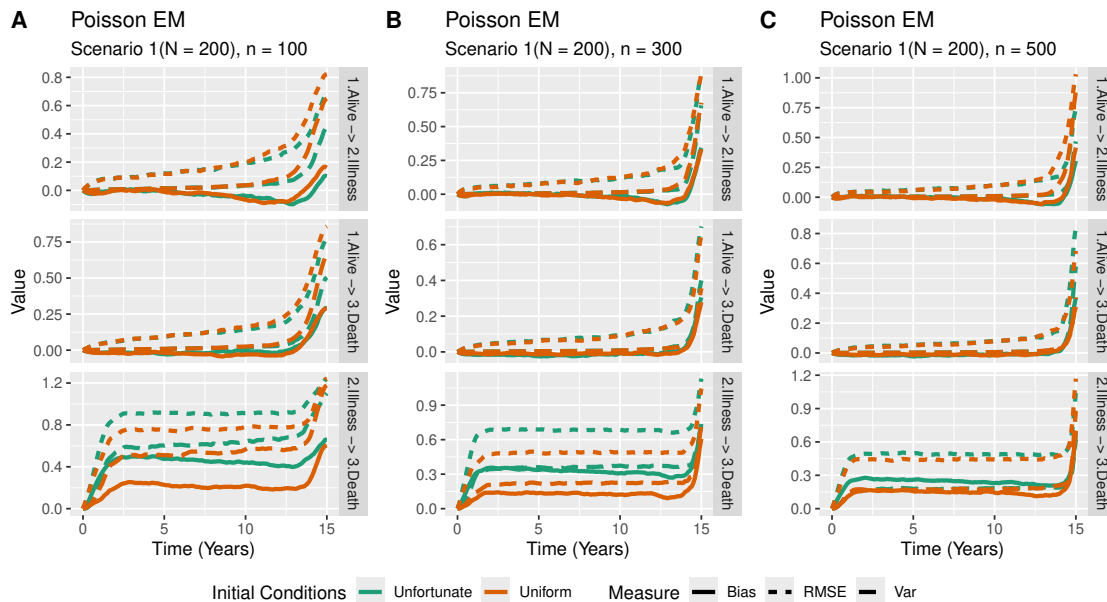


Figure 3: Bias, Variance and RMSE of cumulative intensities in scenario 1 with A)  $n = 100$ , B)  $n = 300$ , C)  $n = 500$  subjects in  $N = 200$  simulated data sets. Only Poisson EM is considered, with uniform and “unfortunate” initial conditions.

As expected, the time-homogeneous model does not recover the underlying form of the hazards at all. We observe the same behaviour as in Scenario 1, where the cumulative intensities seem to be more appropriately recovered by the latent Poisson approach, whereas the transition probabilities are recovered equally well by the two EM methods. All in all, the estimates are unreliable when only very few transitions are observed (early and late study times).

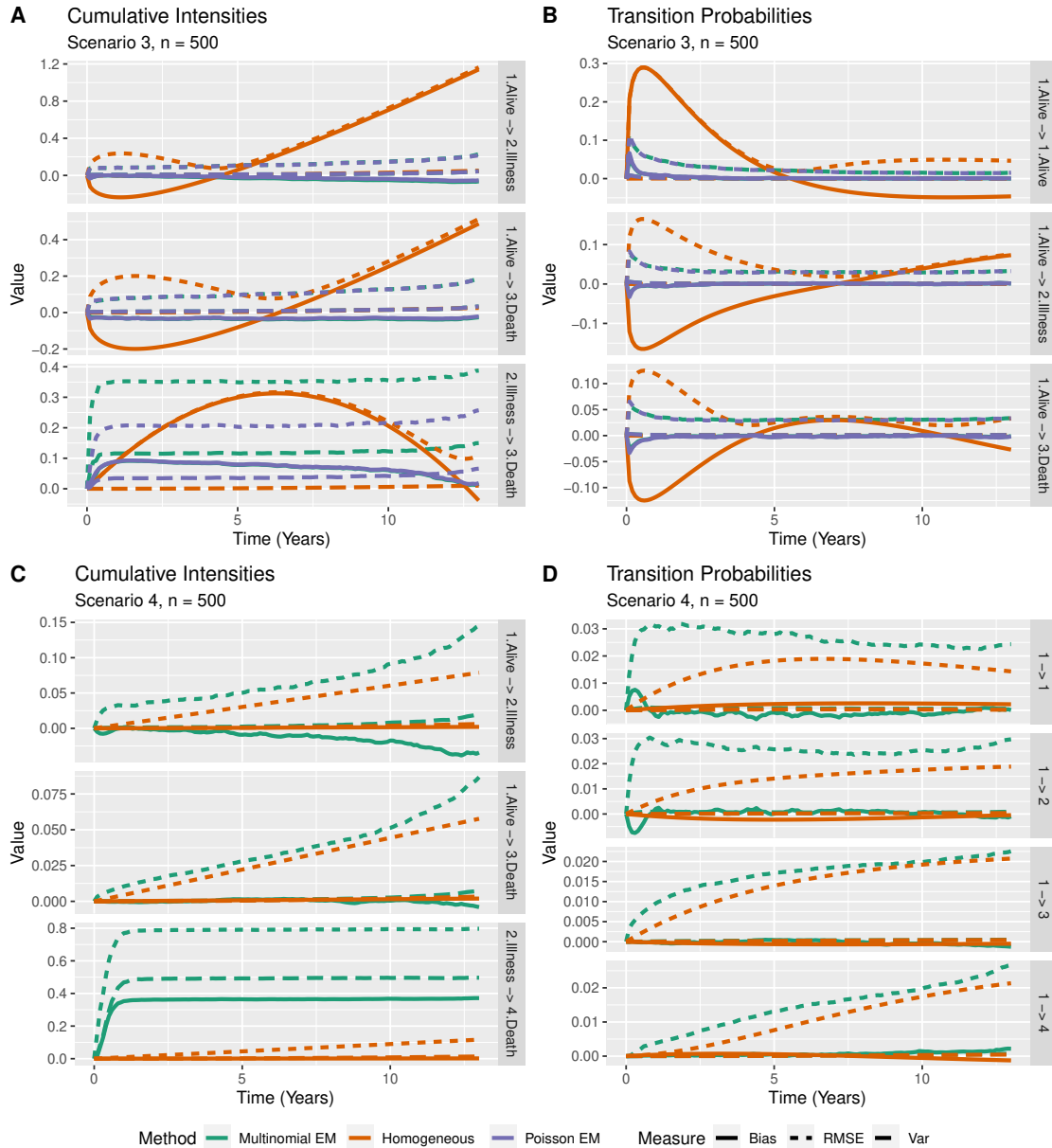


Figure 4: Bias, Variance and RMSE of cumulative intensities/transition probabilities for  $n = 500$  subjects in A-B) scenario 3 and C-D) scenario 4.

### 3.2.4 Scenario 4

In this scenario we consider the extended illness-death model with both death states exactly observed. We compare only the multinomial EM method with the time-homogeneous approach, as the latent Poisson approach was not worked out for this case. Note that the `msm` package allows for the inclusion of exactly observed states. The underlying hazards were therefore chosen to be exponential so that a comparison between the methods can be made. The results for  $n = 500$  can be found in Figure 4 C-D.

Both methods recover the transition probabilities from the initial state very well. The cumulative intensity estimate suffers from the same issues as in scenarios 1 and 3. The RMSE of the multinomial estimator is very similar to the well specified time-homogeneous model. In conclusion, we recover the intensities well even in the case of exactly observed states.

### 3.2.5 Computation speed

A critical attribute of a method is whether it can be used on real-life data sets. The time required to obtain estimates plays a major role therein. Both EM approaches require the calculation of the same number of product integrals per iterations, and these calculations make up the largest part of the total computation time. Each iteration therefore takes roughly the same time for both approaches. To compare the two approaches, the mean number of iterations (and standard deviation) required to reach convergence over the  $N = 1000$  repeats in scenario 3 is shown in Table 2. The Poisson approach requires significantly more iterations to reach convergence than our proposed method and was therefore much slower in our experience. To put time in perspective, it took the multinomial EM algorithm on average 6.5 minutes to reach convergence on a data set with  $n = 500$  using a single core of the 2.6Ghz Intel Xeon Gold 6126 processor as opposed to 21 minutes for the Poisson algorithm.

EM algorithm	Sample size		
	100	300	500
Multinomial	331(155)	474(162)	513(128)
Poisson	549(230)	684(202)	702(210)

Table 2: Mean number of iterations (standard deviation) required to reach convergence over the  $N = 1000$  data sets in scenario 3 for the two EM algorithms.

The time-homogeneous approach implemented in the `msm` package was extremely fast in the first three scenarios, taking less than a minute to run all simulations. In scenario 4 however, the homogeneous approach took about twice as long as the multinomial EM algorithm. This happens because `msm` uses the standard optimisation routine in R to maximise the observed-data likelihood, which is very slow when the (derivative of the) likelihood becomes hard to evaluate.

In conclusion, when all non-absorbing states are covered by the starting state, both EM approaches seem to produce consistent estimates. The latent Poisson approach was also developed for semi-parametric estimation, allowing for the incorporation of covariates and random effects, but does not allow to obtain interpretable estimates when all subjects start in a single state. The multinomial approach yields interpretable estimates when all subjects start in a single state, and is comparatively fast. The time-homogeneous approach is fast, accurate and can implement covariate effects, but is very restrictive for the underlying form of the hazard functions and loses its computational advantage when the data becomes more complicated (such as exactly observed transitions).

## 4 Application

In this section, we analyse a part of the Signal-Tandmobiel study (described in Vanobbergen et al.)[18] using an appropriate multi-state model.

### 4.1 Signal Tooth study data description

The Signal-Tandmobiel study contains longitudinal information on the occurrence of permanent teeth, caries as well as other (oral) descriptive characteristics between 1996 and 2001 for 4430 children born in 1989. The data set is freely available from the R package `icensBKL` [1]. Children were examined at most six times per year, with emergence and caries status being determined through inspection by a dentist leading to panel data. All children start with only deciduous teeth (no permanent teeth). As the interest lies in a non-parametric approach, we leave out any covariate information. Instead, we focus on the emergence and caries status of spatially close permanent teeth 44 and 46. Clearly, a tooth must first emerge before caries can develop. We therefore consider the model shown in Figure 1b, with D indicating deciduous teeth only, P a permanent tooth and C a permanent tooth with caries. Only a single child had tooth 44 emerge before tooth 46, therefore this child was removed from the study in order to significantly simplify the model. Although no formal comparison can be made, we are interested in investigating whether caries on tooth 46 accelerates the occurrence of permanent tooth 44. Besides this, we also take a look at the difference in the occurrence of caries on tooth 46 between different pathways.

For the analysis, we fit the considered model using the multinomial and latent Poisson approach. The EM algorithms were run until the difference in the estimated intensities was smaller than 0.0001 and the homogeneous model was run with initial estimates determined by the `msm` function. Additionally, a time-homogeneous model with piecewise-constant intensities was also considered. Due to numerical issues, the model was simplified to not include states 6 and

7. As no transitions were observed before 6 years of age, the cut-points for the homogeneous model were chosen at 6, 8 and 10 years to split the relevant time-frame into three equal parts.

## 4.2 Results

It took the multinomial algorithm 509 iterations ( $\approx 2$  hours) to converge, whereas the Poisson EM algorithm had not converged yet within the first 4000 iterations and was stopped after 18 hours. Although stopped prematurely, the resulting estimates did not differ much between the latent Poisson and multinomial approach. On further inspection, we found that the increase in the likelihood value per iteration was substantially smaller for the latent Poisson approach. Due to the small differences, we only show the results for the multinomial EM approach. Transition probabilities from the initial state to all other states can be seen in Figure 5 A. As mentioned before, tooth 46 emerges before 44, with caries on 46 therefore often preceding the emergence of tooth 44. Interestingly, almost none of the children developed caries on both teeth. Additionally, approximately 70 percent of children did not develop caries on any of the 2 considered teeth at the end of the study.

To see whether caries on tooth 46 accelerates the emergence of tooth 44, we plot the cumulative hazards for the transitions  $P46 \rightarrow P44+P46$  and  $C46 \rightarrow P44+C46$  in Figure 5 B. Note that  $C46$  cannot occur before  $P46$ , and  $C46$  per definition implies that  $P44$  has not happened yet therefore we expect the  $C46 \rightarrow P44+C46$  transition to have a delayed increase in the cumulative hazard. We can see however that the opposite is true for both models, with the cumulative hazard for the emergence of tooth 44 being larger if caries is first observed on tooth 46, giving rise to the belief that caries does indeed accelerate the occurrence of  $P44$ . This is perhaps a bit surprising, as an earlier analysis has shown that occlusal plaque (which usually precedes the occurrence of caries) on tooth 46 has no effect on the emergence of tooth 44 (see Example 4.2 of Bogaerts et al. [1]).

The cumulative hazards of the two most common pathways to caries on tooth 46 are shown in Figure 5 C. A similar issue is also present here, as  $P46$  must precede the caries-free state  $P44+P46$  and therefore we expect the rate of caries occurrence from the second state to increase at a later time point. The overall slopes of the multinomial EM estimates suggest that neither of the two pathways considered is associated with an increased risk of developing caries. The observed increase in the slope for the second transition can be attributed to the smaller risk set at age 8, as a small risk set may lead to large jumps in the estimated cumulative hazard whenever caries is observed. The homogeneous estimates for the two transitions are comparable, with the two transitions displaying similar slopes but shifted in time. Although the same conclusion is reached using the two methods, the homogeneous approach requires the specification of cut-points. Such a choice requires manual analysis of the data set, in contrast to the EM approaches.

## 5 Discussion

We have derived a non-parametric maximum likelihood estimator for the transition intensities in multi-state models without loops for a combination of interval- and right-censored data. The estimator makes use of the Expectation-maximisation algorithm and is based on the multinomial complete data likelihood for panel data. We present a necessary and sufficient condition to determine convergence of the algorithm to the true NPMLE. The estimated quantities allow to determine (cumulative) hazards for any transition in the model, as well as transition probabilities over the study period.

In comparison with the latent Poisson EM estimator [15], which was shown to be consistent for the cumulative intensities, our approach yielded almost identical estimates when the initial state can be any non-absorbing state. Additionally, our estimator yielded interpretable estimates for the transition probabilities when all subjects were initially observed in a single state, contrary to the latent Poisson approach. Finally, the multinomial EM algorithm was found to need significantly less iterations to converge at an estimator, making this approach computationally feasible.

In contrast to the time-homogeneous approach, the underlying cumulative intensities can be modelled with much greater flexibility. Additionally, in the presence of exactly observed (right-censored) states, our approach is computationally faster than existing time-homogeneous implementations as it does not rely on numerical optimisation techniques.

The multinomial and latent Poisson EM estimators allow for the proper analysis of interval-censored panel data, negating the need to use inappropriate or incorrectly specified models. This in turn yields interpretable estimates and allows for unbiased conclusions in the presence of interval-censoring.

An important consideration when using the proposed estimator is the conditionally independent visit assumption. If future visit times are not independent of the state of the subject since the last visit, the proposed estimator might

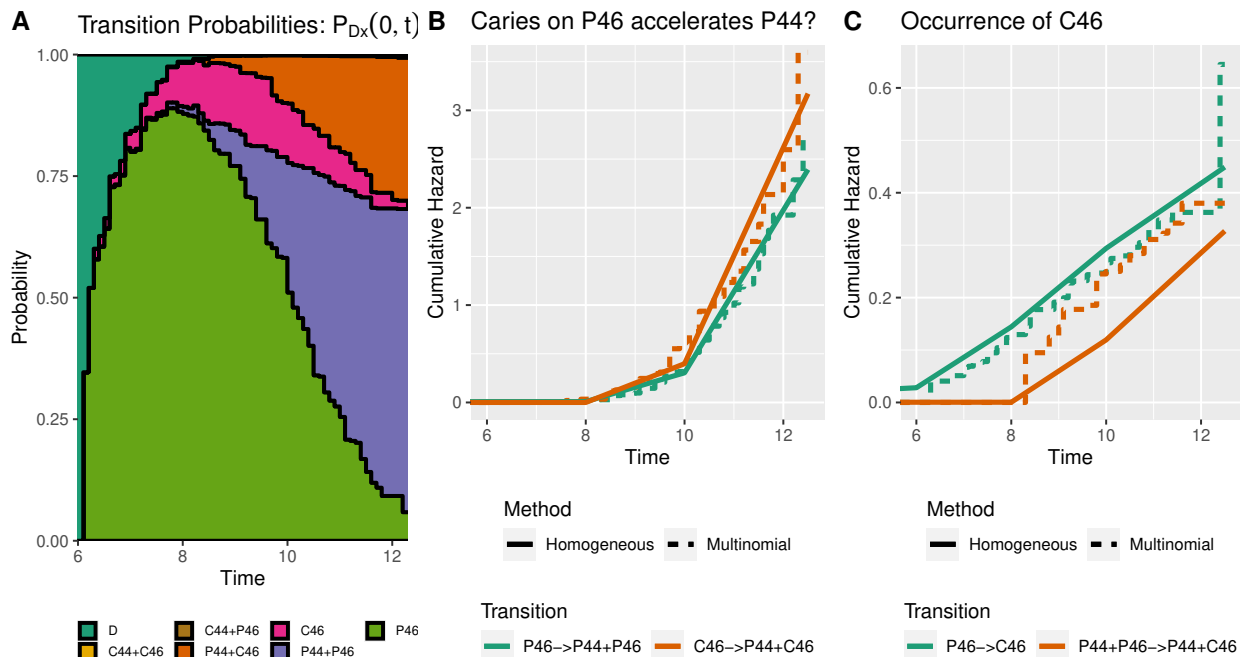


Figure 5: A) Transition probabilities (multinomial EM) from initial state D over time. The height of a colour indicates the probability of being in the corresponding state. B) Comparison of occurrence of permanent tooth 44 with or without caries on permanent tooth 46. C) Occurrence of caries on tooth 46 through the two most common pathways.

produce biased estimates. This problem may occur in the commonly used illness-death model, where sometimes subjects are more likely to visit a doctor shortly after contracting the disease.

Although a condition was derived to determine whether the algorithm has converged towards the NPMLE, the NPMLE might not exist or not be unique [17, 25]. The NPMLE may not be unique when the complete data log-likelihood function (Equation (5)) is not strictly concave. For the standard survival setting, a sufficient condition for the uniqueness of the NPMLE is given in Gentleman & Geyer [17]. A similar condition could be derived for panel data as well.

The proposed estimator yields virtually identical estimates as the latent Poisson approach, thereby implying consistent estimation of the cumulative intensities. A theoretical confirmation of this presumption could be derived following the procedure in Gu et al. [15]. Furthermore, the potential extension of our estimator to the semi-parametric framework via a proportional hazards approach should be considered. In a semi-parametric approach, a hypothesis test of a zero regression coefficient has been used to compare survival curves in an interval-censored setting [26]. A similar approach could also be used for panel data, and would allow us to formally compare the cumulative intensities in the Signal Tandmobiel study.

Asymptotic properties of the introduced estimator were not discussed in this article. For the right-censored time to event case we quote Hudgens et al. [25]: “If the support of the censoring mechanism is discrete and finite, the estimation of the cumulative incidence functions becomes a finite dimensional estimation problem and we expect the NPMLE to have the usual  $n^{1/2}$  convergence rate. If the random variables dictating the censoring are treated as continuous, the rate of convergence of the NPMLE will likely not be  $n^{1/2}$ , and derivation of the limiting distribution will not be trivial.” We expect the same to hold in the case of panel data, as the latent Poisson estimator has been shown to have a convergence rate of  $n^{1/3}$  in the case of continuously distributed censoring.[16]

In panel data, the state of a subject at a visit time is sometimes only known to lie in a set of possible states. It is possible to consider this extension to our model as well, following existing results for the time-homogeneous model [9]. Furthermore, extensions for truncated data should be considered.

## 6 Acknowledgements

This work was performed using the ALICE compute resources provided by Leiden University.

## 7 Software

Software to determine the NPMLE for a general multi-state model without loops is freely available in the R package `icmstate` on GitHub at [github.com/d-gomon/icmstate](https://github.com/d-gomon/icmstate).

## References

- [1] K. Bogaerts, A. Komárek, and E. Lesaffre. *Survival Analysis with Interval-Censored data*. Taylor & Francis Group, 2020.
- [2] B. W. Turnbull. The empirical distribution function with arbitrarily grouped, censored and truncated data. *Journal of the Royal Statistical Society: Series B (Methodological)*, 38(3):290–295, July 1976.
- [3] J. C. Lindsey and L. M. Ryan. Methods for interval-censored data. *Statistics in Medicine*, 17(2):219–238, January 1998.
- [4] D. Commenges. Inference for multi-state models from interval-censored data. *Statistical Methods in Medical Research*, 11(2):167–182, April 2002.
- [5] O. O. Aalen and S. Johansen. An empirical transition matrix for non-homogeneous Markov chains based on censored observations. *Scandinavian Journal of Statistics*, 5:141–150, 1978.
- [6] R. J. Cook and J. F. Lawless. *Multistate Models for the Analysis of Life History Data*. Taylor & Francis Group, 2020.
- [7] P. K. Andersen and H. Ravn. *Models for Multi-State Survival Data: Rates, Risks, and Pseudo-Values*. CRC Press, 2024.
- [8] H. Putter, M. Fiocco, and R. B. Geskus. Tutorial in biostatistics: competing risks and multi-state models. *Statistics in Medicine*, 26(11):2389–2430, October 2006.
- [9] C. H. Jackson. Multi-state models for panel data: The `msm` package for R. *Journal of Statistical Software*, 38(8), 2011.
- [10] R. C. Gentleman, J. F. Lawless, J. C. Lindsey, and P. Yan. Multi-state Markov models for analysing incomplete disease history data with illustrations for HIV disease. *Statistics in Medicine*, 13(8):805–821, April 1994.
- [11] H. Frydman. A nonparametric estimation procedure for a periodically observed three-state Markov process, with application to Aids. *Journal of the Royal Statistical Society: Series B (Methodological)*, 54(3):853–866, July 1992.
- [12] H. Frydman. Nonparametric estimation of a Markov ‘illness-death’ process from interval-censored observations, with application to diabetes survival data. *Biometrika*, 82(4):773, December 1995.
- [13] P. Joly. A penalized likelihood approach for an illness-death model with interval-censored data: application to age-specific incidence of dementia. *Biostatistics*, 3(3):433–443, September 2002.
- [14] R. J. M. Machado and A. van den Hout. Flexible multistate models for interval-censored data: Specification, estimation, and an application to ageing research. *Statistics in Medicine*, 37(10):1636–1649, January 2018.
- [15] Y. Gu, D. Zeng, G. Heiss, and D. Y. Lin. Maximum likelihood estimation for semiparametric regression models with interval-censored multistate data. *Biometrika*, November 2023.
- [16] Y. Gu. *Statistical methods for analyzing interval-censored multi-state data*. PhD thesis, University of North Carolina at Chapel Hill, 2023.
- [17] R. Gentleman and C. J. Geyer. Maximum likelihood for interval censored data: Consistency and computation. *Biometrika*, 81(3):618–623, 1994.
- [18] J. Vanobbergen, L. Martens, E. Lesaffre, and D. Declerck. The Signal-Tandmobiel® project, a longitudinal intervention health promotion study in Flanders (Belgium): baseline and first year results. *European Journal of Paediatric Dentistry*, 2:87–96, 2000.
- [19] A. P. Dempster, N. M. Laird, and D. B. Rubin. Maximum likelihood from incomplete data via the EM algorithm. *Journal of the Royal Statistical Society: Series B (Methodological)*, 39(1):1–22, September 1977.
- [20] W. Nelson. Hazard plotting for incomplete failure data. *Journal of Quality Technology*, 1(1):27–52, January 1969.
- [21] O. Aalen. Nonparametric inference for a family of counting processes. *The Annals of Statistics*, 6(4), July 1978.
- [22] S. P. Boyd and L. Vandenberghe. *Convex optimization*. Cambridge University Press, 2023.

- [23] Y. Ma and Y. Wang. Efficient distribution estimation for data with unobserved sub-population identifiers. *Electronic Journal of Statistics*, 6, Jan 2012.
- [24] R Core Team. *R: A Language and Environment for Statistical Computing*. R Foundation for Statistical Computing, Vienna, Austria, 2020.
- [25] M. G. Hudgens, G. A. Satten, and I. M. Longini. Nonparametric maximum likelihood estimation for competing risks survival data subject to interval censoring and truncation. *Biometrics*, 57(1):74–80, March 2001.
- [26] D. M. Finkelstein. A proportional hazards model for interval-censored failure time data. *Biometrics*, 42(4):845, December 1986.



---

SUPPLEMENTAL MATERIAL TO NON-PARAMETRIC ESTIMATION  
OF TRANSITION INTENSITIES IN INTERVAL CENSORED  
MARKOVIAN MULTI-STATE MODELS WITHOUT LOOPS

---

Daniel Gomon <sup>1,\*</sup>, Hein Putter <sup>1,2</sup>

<sup>1</sup> *Mathematical Institute, Leiden University, Einsteinweg 55, Leiden, the Netherlands*

<sup>2</sup> *Department of Biomedical Data Sciences, Leiden University Medical Centre, Einthovenweg 20, Leiden, the Netherlands*

### A Notation Visualisation

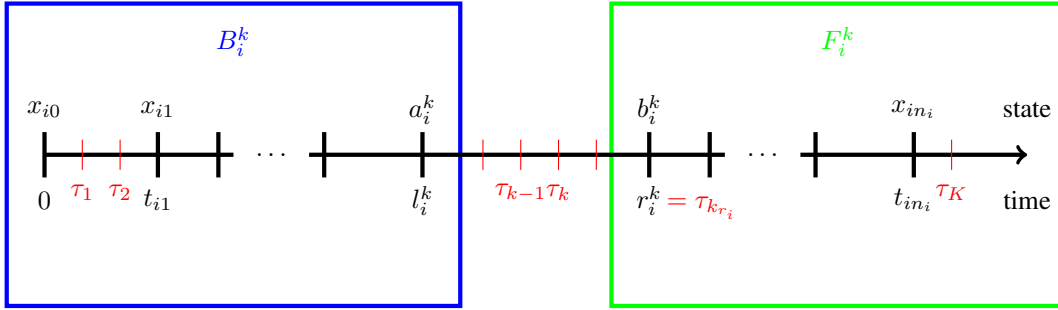


Figure 1: Graphical representation of data notation for a single subject  $i$  and fixed  $k \in \{1, \dots, K\}$ .

### B Derivations for the EM algorithm

#### B.1 Panel data

**Proposition 1** *Consider the conditional expectation of the complete data log-likelihood function for panel data:*

$$\mathbb{E}[\ell^C | \mathbf{O}, \tilde{\alpha}] = \sum_{k=1}^K \sum_{(g,h) \in \mathcal{V}} \{ \mathbb{E} [d_{gh}^k | \mathbf{O}, \tilde{\alpha}] \log(\alpha_{gh}^k) - \alpha_{gh}^k \mathbb{E} [Y_g^k | \mathbf{O}, \tilde{\alpha}] \}. \quad (1)$$

*The following conditional expectations when no transition times are known exactly are given by:*

$$d_{gh}^k(\tilde{\alpha}) := \mathbb{E} [d_{gh}^k | \mathbf{O}, \tilde{\alpha}] = \sum_{i=1}^n \frac{\tilde{P}_{a_i^k, g}(l_i^k, \tau_{k-1}) \cdot \tilde{\alpha}_{gh, k} \cdot \tilde{P}_{h, b_i^k}(\tau_k, r_i^k)}{\tilde{P}_{a_i^k, b_i^k}(l_i^k, r_i^k)},$$

$$Y_g^k(\tilde{\alpha}) := \mathbb{E} [Y_g^k | \mathbf{O}, \tilde{\alpha}] = \sum_{i=1}^n \frac{\tilde{P}_{a_i^k, g}(l_i^k, \tau_{k-1}) \cdot \tilde{P}_{g, b_i^k}(\tau_k, r_i^k)}{\tilde{P}_{a_i^k, b_i^k}(l_i^k, r_i^k)},$$

*with  $\tilde{\mathbf{P}}(s, t) = \prod_{s < u \leq t} (\mathbf{I} + d\tilde{\mathbf{A}}(u))$  the product integral of the current estimates of the transition intensities.*

---

\*Corresponding Author, d.gomon@math.leidenuniv.nl

*Proof:* For ease of notation, we define  $\tilde{\mathbb{E}}[\cdot] = \mathbb{E}[\cdot|\tilde{\alpha}]$  and  $\tilde{\mathbb{P}}[\cdot] = \mathbb{P}[\cdot|\tilde{\alpha}]$  as the conditional expectation and probability given the current estimates of the transition intensities. As we have assumed that the cumulative intensity is a right-continuous step function with jumps only in  $\mathcal{T}$ , we have:

$$\begin{aligned}\mathbb{E}[d_{gh}^k|O, \tilde{\alpha}] &= \sum_{i=1}^n \mathbb{E}[\mathbb{1}\{X_i(\tau_k) = h, X_i(\tau_k-) = g\}|O, \tilde{\alpha}] \\ &= \sum_{i=1}^n \mathbb{P}(X(\tau_k) = h, X(\tau_k-) = g|\mathbb{X}_i, \tilde{\alpha}) =: \sum_{i=1}^n d_{gh,i}^k(\tilde{\alpha}) =: d_{gh}^k(\tilde{\alpha}), \\ \mathbb{E}[Y_g^k|O, \tilde{\alpha}] &= \sum_{i=1}^n \mathbb{E}[\mathbb{1}\{X_i(\tau_k-) = g\}|O, \tilde{\alpha}] \\ &= \sum_{i=1}^n \mathbb{P}(X(\tau_k-) = g|\mathbb{X}_i, \tilde{\alpha}) =: \sum_{i=1}^n Y_{g,i}^k(\tilde{\alpha}) =: Y_g^k(\tilde{\alpha}),\end{aligned}$$

with  $\tau_k-$  the time just before  $\tau_k$ . Fix some  $k \in \{1, \dots, K\}$  and  $i \in \{1, \dots, n\}$ . Define  $\tilde{F}_i^k = F_i^k \setminus \{X_i(r_i^k)\}$  and  $\tilde{B}^K = B_i^k \setminus \{X_i(l_i^k)\}$ . We leave away the subscript  $i$  when possible to simplify notation below. We look at the individual terms separately:

$$\begin{aligned}Y_{g,i}^k(\tilde{\alpha}) &= \tilde{\mathbb{P}}(X(\tau_k-) = g|\mathbb{X}_i) \\ &= \tilde{\mathbb{P}}(X(\tau_k-) = g|\tilde{B}^K, X(l_i^k) = a_i^k, X(r_i^k) = b_i^k, \tilde{F}^k) \\ &= \frac{\tilde{\mathbb{P}}(X(r_i^k) = b_i^k, \tilde{F}^k|X(\tau_k-) = g, \tilde{B}^K, X(l_i^k) = a_i^k) \cdot \tilde{\mathbb{P}}(X(\tau_k-) = g|\tilde{B}^K, X(l_i^k) = a_i^k)}{\tilde{\mathbb{P}}(X(r_i^k) = b_i^k, \tilde{F}^k|X(l_i^k) = a_i^k, \tilde{B}^K)} \\ &\stackrel{Markov}{=} \frac{\tilde{\mathbb{P}}(X(r_i^k) = b_i^k, \tilde{F}^k|X(\tau_k-) = g) \cdot \tilde{\mathbb{P}}(X(\tau_k-) = g|X(l_i^k) = a_i^k)}{\tilde{\mathbb{P}}(X(r_i^k) = b_i^k, \tilde{F}^k|X(l_i^k) = a_i^k)} \\ &= \frac{\tilde{\mathbb{P}}(\tilde{F}^k|X(r_i^k) = b_i^k, X(\tau_k-) = g) \cdot \tilde{\mathbb{P}}(X(r_i^k) = b_i^k|X(\tau_k-) = g) \cdot \tilde{\mathbb{P}}(X(\tau_k-) = g|X(l_i^k) = a_i^k)}{\tilde{\mathbb{P}}(\tilde{F}^k|X(r_i^k) = b_i^k, X(\tau_k-) = g) \cdot \tilde{\mathbb{P}}(X(r_i^k) = b_i^k|X(l_i^k) = a_i^k)} \\ &\stackrel{Markov}{=} \frac{\tilde{\mathbb{P}}(X(r_i^k) = b_i^k|X(\tau_k-) = g) \cdot \tilde{\mathbb{P}}(X(\tau_k-) = g|X(l_i^k) = a_i^k)}{\tilde{\mathbb{P}}(X(r_i^k) = b_i^k|X(l_i^k) = a_i^k)} \\ &= \frac{\tilde{P}_{a_i^k, g}(l_i^k, \tau_k-) \cdot \tilde{P}_{g, b_i^k}(\tau_k-, r_i^k)}{\tilde{P}_{a_i^k, b_i^k}(l_i^k, r_i^k)},\end{aligned}\tag{2}$$

with  $\tilde{P}_{gh}(s, t)$  the  $(g, h)$ -th entry of the product integral over the current estimates  $\tilde{\mathbf{P}}(s, t) = \prod_{s < u \leq t} (\mathbf{I} + d\tilde{\mathbf{A}}(u))$ .

We continue to the next term:

$$\begin{aligned}d_{gh,i}^k &= \tilde{\mathbb{P}}(X(\tau_k-) = g, X(\tau_k) = h|\mathbb{X}_i) \\ &= \tilde{\mathbb{P}}(X(\tau_k-) = g|\mathbb{X}_i) \cdot \tilde{\mathbb{P}}(X(\tau_k) = h|X(\tau_k-) = g, \mathbb{X}_i).\end{aligned}\tag{3}$$

The first term is simply  $Y_{g,i}^k(\tilde{\alpha})$ , so we take a further look at the second term:

$$\begin{aligned}\tilde{\mathbb{P}}(X(\tau_k) = h|X(\tau_k-) = g, \mathbb{X}_i) &= \frac{\tilde{\mathbb{P}}(X(\tau_k) = h, X(\tau_k-) = g, B^k, F^k)}{\tilde{\mathbb{P}}(X(\tau_k-) = g, B^k, F^k)} \\ &= \frac{\tilde{\mathbb{P}}(F^k|X(\tau_k) = h) \cdot \tilde{\mathbb{P}}(X(\tau_k) = h|X(\tau_k-) = g)}{\tilde{\mathbb{P}}(F^k|X(\tau_k-) = g)} \\ &= \frac{\tilde{\mathbb{P}}(X(r_i^k) = b_i^k|X(\tau_k) = h) \cdot \tilde{\alpha}_{gh}^k}{\tilde{\mathbb{P}}(X(r_i^k) = b_i^k|X(\tau_k-) = g)} \\ &= \frac{\tilde{\mathbb{P}}(X(r_i^k) = b_i^k|X(\tau_k) = h) \cdot \tilde{\alpha}_{gh}^k}{\tilde{\mathbb{P}}(X(r_i^k) = b_i^k|X(\tau_k-) = g)} \\ &= \frac{\tilde{P}_{h, b_i^k}(\tau_k, r_i^k) \cdot \tilde{\alpha}_{gh}^k}{\tilde{P}_{g, b_i^k}(\tau_k-, r_i^k)}.\end{aligned}\tag{4}$$

As the cumulative intensities were assumed to be right-continuous step functions, we obtain that:

$$\tilde{P}_{gh}(\tau_k-, t) = \tilde{P}_{gh}(\tau_{k-1}, t)$$

for any  $k \in 1, \dots, K$  and any  $t > \tau_k$ . Using this fact and substituting Equations (4) and (2) into Equation (3) and summing over  $n$  we obtain the final result.  $\square$

**Proposition 2** *The conditional expected value of the complete data log-likelihood for panel data (see Equation (1)) over the optimisation region:*

$$C_\alpha = \left\{ \alpha_{gh}^k, g, h \in \mathcal{H}, k = 1, \dots, K; \alpha_{gh}^k \geq 0, \sum_{h \neq g=1}^H \alpha_{gh}^k \leq 1 \right\},$$

is maximised by the following expression:

$$\alpha_{gh}^k = \begin{cases} \frac{d_{gh}^k(\tilde{\alpha})}{Y_g^k(\tilde{\alpha})}, & \mu_g^k = 0, \\ \frac{d_{gh}^k(\tilde{\alpha})}{\sum_{h \leftarrow g} d_{gh}^k(\tilde{\alpha})}, & \mu_g^k > 0. \end{cases}$$

*Proof:* Maximisation of the complete data log-likelihood function can be phrased as a convex optimization problem. The primal problem is given by (denoting  $l^C(\alpha) = \mathbb{E}[l^C]$ ):

$$\begin{aligned} \max \quad & l^C(\alpha) = \sum_{k=1}^K \sum_{(g,h) \in \mathcal{V}} d_{gh}^k(\tilde{\alpha}) \log(\alpha_{gh}^k) - \sum_{k=1}^K \sum_{(g,h) \in \mathcal{V}} \alpha_{gh}^k Y_g^k(\tilde{\alpha}) \\ \text{s.t.} \quad & \alpha_{gh}^k \geq 0, & g, h \in \mathcal{H}, k \in \{1, \dots, K\}, \\ & \sum_{h \neq g} \alpha_{gh}^k \leq 1, & g \in \mathcal{H}, k \in \{1, \dots, K\}, \end{aligned}$$

or rewritten as a minimization problem:

$$\begin{aligned} \min \quad & -l^C(\alpha) = \sum_{k=1}^K \sum_{(g,h) \in \mathcal{V}} \alpha_{gh}^k Y_g^k(\tilde{\alpha}) - \sum_{k=1}^K \sum_{(g,h) \in \mathcal{V}} d_{gh}^k(\tilde{\alpha}) \log(\alpha_{gh}^k) \\ \text{s.t.} \quad & -\alpha_{gh}^k \leq 0, & g, h \in \mathcal{H}, k \in \{1, \dots, K\}, \\ & \sum_{h \neq g} \alpha_{gh}^k - 1 \leq 0, & g \in \mathcal{H}, k \in \{1, \dots, K\}. \end{aligned}$$

As the logarithm is a concave function, minus the logarithm is convex and the addition of linear terms results in a convex function  $-l^C(\alpha)$ . The Lagrangian is given by:

$$\begin{aligned} \mathcal{L}(\alpha, \mu, \lambda) = & \sum_{k=1}^K \sum_{(g,h) \in \mathcal{V}} \alpha_{gh}^k Y_g^k(\tilde{\alpha}) - \sum_{k=1}^K \sum_{(g,h) \in \mathcal{V}} d_{gh}^k(\tilde{\alpha}) \log(\alpha_{gh}^k) \\ & - \sum_{g=1}^H \sum_{h \neq g} \sum_{k=1}^K \lambda_{gh}^k \alpha_{gh}^k + \sum_{g=1}^H \sum_{k=1}^K \mu_g^k \left( \sum_{h \neq g=1}^H \alpha_{gh}^k - 1 \right), \end{aligned}$$

with  $\lambda_{gh}^k, \mu_g^k$  called Lagrange multipliers. A necessary and sufficient condition for  $\alpha$  to be a (local) minimum to above minimisation problem is given by the Karush-Kuhn-Tucker (KKT) conditions (See Section 5.5.3 of [?]):

$$\begin{aligned} (1) \quad & \frac{\partial \mathcal{L}(\alpha, \mu)}{\partial \alpha_{gh}^k} = Y_g^k - \frac{d_{gh}^k}{\alpha_{gh}^k} - \lambda_{gh}^k + \mu_g^k = 0, & g \neq h \in \mathcal{H}, k \in \{1, \dots, K\}, \\ (2) \quad & \lambda_{gh}^k \alpha_{gh}^k = 0, & g \neq h \in \mathcal{H}, k \in \{1, \dots, K\}, \\ (3) \quad & \mu_g^k \left( \sum_{h \leftarrow g} \alpha_{gh}^k - 1 \right) = 0, & g \in \mathcal{H}, k \in \{1, \dots, K\}, \\ (4) \quad & \alpha_{gh}^k \geq 0, & g, h \in \mathcal{H}, k \in \{1, \dots, K\}, \\ (5) \quad & \sum_{h \leftarrow g} \alpha_{gh}^k - 1 \leq 0, & g \in \mathcal{H}, k \in \{1, \dots, K\}, \\ (6) \quad & \lambda_{gh}^k, \mu_g^k \geq 0, & g, h \in \mathcal{H}, k \in \{1, \dots, K\}. \end{aligned}$$

When  $\sum_{h \neq g=1}^H \alpha_{gh}^k - 1 < 0$ , constraint (3) is called inactive. When the constraint is inactive, we must have that  $\mu_g^k = 0$ . When the constraint is active,  $\mu_g^k$  tells us how much we can improve the objective function by changing the right-hand side of the inequality constraint. Note that  $\mu_g^k$  must be positive, as increasing the right hand side of inequality constraint (5) can improve the objective function.

From equality (1) in the KKT conditions we recover:

$$Y_g^k(\tilde{\alpha}) - \frac{d_{gh}^k(\tilde{\alpha})}{\alpha_{gh}^k} - \lambda_{gh}^k + \mu_g^k = 0.$$

Note that this is undefined for  $\alpha_{gh}^k = 0$ . Clearly, if  $d_{gh}^k(\tilde{\alpha}) = 0$ , then such a transition is not possible under our current estimate of  $\alpha$ , so we define  $\frac{0}{0} = 0$ . Suppose that  $\alpha_{gh}^k > 0$ . In that case, the complementary slackness condition  $\lambda_{gh}^k \alpha_{gh}^k = 0$  ensures that  $\lambda_{gh}^k = 0$ . We obtain:

$$Y_g^k(\tilde{\alpha}) - \frac{d_{gh}^k(\tilde{\alpha})}{\alpha_{gh}^k} + \mu_g^k = 0. \quad (5)$$

Multiply both sides by  $\alpha_{gh}^k > 0$ :

$$\alpha_{gh}^k Y_g^k(\tilde{\alpha}) - d_{gh}^k(\tilde{\alpha}) + \alpha_{gh}^k \mu_g^k = 0.$$

Sum over all states  $h$  directly connected to  $g$ :

$$Y_g^k(\tilde{\alpha}) \sum_{h \leftarrow g} \alpha_{gh}^k - \sum_{h \leftarrow g} d_{gh}^k(\tilde{\alpha}) + \mu_g^k \sum_{h \leftarrow g} \alpha_{gh}^k = 0.$$

We add and subtract  $\mu_g^k$  to obtain:

$$Y_g^k(\tilde{\alpha}) \sum_{h \leftarrow g} \alpha_{gh}^k - \sum_{h \leftarrow g} d_{gh}^k(\tilde{\alpha}) + \mu_g^k \left( \sum_{h \leftarrow g} \alpha_{gh}^k - 1 \right) + \mu_g^k = 0,$$

and using KKT Condition (3):

$$\mu_g^k = \sum_{h \leftarrow g} d_{gh}^k(\tilde{\alpha}) - Y_g^k(\tilde{\alpha}) \sum_{h \leftarrow g} \alpha_{gh}^k.$$

Finally, we obtain:

$$\sum_{h \leftarrow g} \alpha_{gh}^k = \frac{-\mu_g^k + \sum_{h \leftarrow g} d_{gh}^k(\tilde{\alpha})}{Y_g^k(\tilde{\alpha})}. \quad (6)$$

Alternatively, we rewrite Equation (5) to obtain:

$$\alpha_{gh}^k = \frac{d_{gh}^k(\tilde{\alpha})}{Y_g^k(\tilde{\alpha}) + \mu_g^k}, \quad (7)$$

and summing over  $h \leftarrow g$ :

$$\sum_{h \leftarrow g} \alpha_{gh}^k = \frac{\sum_{h \leftarrow g} d_{gh}^k(\tilde{\alpha})}{Y_g^k(\tilde{\alpha}) + \mu_g^k}. \quad (8)$$

Now equating Equations (6) and (8) we obtain:

$$\frac{-\mu_g^k + \sum_{h \leftarrow g} d_{gh}^k(\tilde{\alpha})}{Y_g^k(\tilde{\alpha})} = \frac{\sum_{h \leftarrow g} d_{gh}^k(\tilde{\alpha})}{Y_g^k(\tilde{\alpha}) + \mu_g^k}.$$

After some algebra we obtain:

$$\mu_g^k \left( \mu_g^k + Y_g^k(\tilde{\alpha}) - \sum_{h \leftarrow g} d_{gh}^k(\tilde{\alpha}) \right) = 0.$$

Taking into account that  $\mu_g^k \geq 0$  for a feasible solution, we must have:

$$\mu_g^k = \max \left( 0, \sum_{h \leftarrow g} d_{gh}^k(\tilde{\alpha}) - Y_g^k(\tilde{\alpha}) \right). \quad (9)$$

Substituting Equation (9) into Equation (7) we obtain the final result:

$$\alpha_{gh}^k = \begin{cases} \frac{d_{gh}^k(\tilde{\alpha})}{Y_g^k(\tilde{\alpha})}, & \mu_g^k = 0, \\ \frac{d_{gh}^k(\tilde{\alpha})}{\sum_{h \leftarrow g} d_{gh}^k(\tilde{\alpha})}, & \mu_g^k > 0. \end{cases} \quad (10)$$

□

## B.2 Panel data with exactly observed states

**Proposition 3** Consider the conditional expectation of the complete data log-likelihood function for panel data:

$$\mathbb{E}[\ell^C | \mathbf{O}, \tilde{\alpha}] = \sum_{k=1}^K \sum_{(g,h) \in \mathcal{V}} \{ \mathbb{E} [d_{gh}^k | \mathbf{O}, \tilde{\alpha}] \log(\alpha_{gh}^k) - \alpha_{gh}^k \mathbb{E} [Y_g^k | \mathbf{O}, \tilde{\alpha}] \}. \quad (11)$$

The conditional expectations for panel data with transition times exactly known for a subset of states  $\mathcal{E} \subseteq \mathcal{H}$  are given by:

$$d_{gh,i}^k(\tilde{\alpha}) := \mathbb{E} [d_{gh,i}^k | \mathbf{O}, \tilde{\alpha}] = \begin{cases} \frac{\tilde{P}_{a_i^k, g}(l_i^k, \tau_{k-1}) \cdot \tilde{\alpha}_{gh, k} \cdot \tilde{P}_{h, b_i^k}(\tau_k, r_i^k)}{\tilde{P}_{a_i^k, b_i^k}(l_i^k, r_i^k)}, & \text{if } b_i^k \notin \mathcal{E} \\ \frac{\tilde{P}_{a_i^k, g}(l_i^k, \tau_{k-1}) \cdot \tilde{\alpha}_{gh}^k \cdot \sum_{m \in \mathcal{R}_{b_i^k}} \tilde{\alpha}_{mb_i^k}^{k_{r_i}} \tilde{P}_{hm}(\tau_k, \tau_{k_{r_i}-1})}{\sum_{m \in \mathcal{R}_{b_i^k}} \tilde{\alpha}_{mb_i^k}^{k_{r_i}} \tilde{P}_{a_i^k m}(l_i^k, \tau_{k_{r_i}-1})}, & \text{if } b_i^k \in \mathcal{E} \end{cases}$$

$$Y_{g,i}^k(\tilde{\alpha}) := \mathbb{E} [Y_{g,i}^k | \mathbf{O}, \tilde{\alpha}] = \begin{cases} \frac{\tilde{P}_{a_i^k, g}(l_i^k, \tau_{k-1}) \cdot \tilde{P}_{g, b_i^k}(\tau_{k-}, r_i^k)}{\tilde{P}_{a_i^k, b_i^k}(l_i^k, r_i^k)}, & \text{if } b_i^k \notin \mathcal{E} \\ \frac{\tilde{P}_{a_i^k, g}(l_i^k, \tau_{k-1}) \cdot \sum_{m \in \mathcal{R}_{b_i^k}} \tilde{\alpha}_{mb_i^k}^{k_{r_i}} \tilde{P}_{gm}(\tau_{k-1}, \tau_{k_{r_i}-1})}{\sum_{m \in \mathcal{R}_{b_i^k}} \tilde{\alpha}_{mb_i^k}^{k_{r_i}} \tilde{P}_{a_i^k m}(l_i^k, \tau_{k_{r_i}-1})}, & \text{if } b_i^k \in \mathcal{E} \end{cases}$$

with  $\tau_{k_{r_i}} := r_i^k$ ,  $d_{gh}^k(\tilde{\alpha}) = \sum_{i=1}^n d_{gh,i}^k(\tilde{\alpha})$ ,  $Y_g^k(\tilde{\alpha}) = \sum_{i=1}^n Y_{g,i}^k(\tilde{\alpha})$  and  $\tilde{\mathbf{P}}(s, t) = \prod_{s < u \leq t} (\mathbf{I} + d\tilde{\mathbf{A}}(u))$  the product integral of the current estimates of the transition intensities.

*Proof:* We follow the beginning of the proof of Proposition 1. Fix  $k$  and  $i$  and consider the situation when  $b_i^k \notin \mathcal{E}$ . It is apparent that the result from Proposition 1 still holds, as no additional information is available in that case. We therefore consider the case when  $b_i^k \in \mathcal{E}$  and look at the individual terms separately:

$$\begin{aligned} Y_{g,i}^k(\tilde{\alpha}) &= \tilde{\mathbb{P}}(X(\tau_k-) = g | \mathbb{X}_i) \\ &= \tilde{\mathbb{P}}(X(\tau_k-) = g | X(r_i^k) = b_i^k, \tilde{B}^K, \tilde{F}^k, X(l_i^k) = a_i^k, b_i^k \in \mathcal{E}) \\ &= \frac{\tilde{\mathbb{P}}(\tilde{F}^k, X(r_i^k) = b_i^k | X(\tau_k-) = g, \tilde{B}^K, X(l_i^k) = a_i^k, b_i^k \in \mathcal{E}) \cdot \tilde{\mathbb{P}}(X(\tau_k-) = g | X(l_i^k) = a_i^k, \tilde{B}^K, b_i^k \in \mathcal{E})}{\tilde{\mathbb{P}}(\tilde{F}^k, X(r_i^k) = b_i^k | X(l_i^k) = a_i^k, \tilde{B}^K, b_i^k \in \mathcal{E})} \\ &\stackrel{\text{Markov}}{=} \frac{\tilde{\mathbb{P}}(\tilde{F}^k, X(r_i^k) = b_i^k | X(\tau_k-) = g, b_i^k \in \mathcal{E}) \cdot \tilde{\mathbb{P}}(X(\tau_k-) = g | X(l_i^k) = a_i^k, b_i^k \in \mathcal{E})}{\tilde{\mathbb{P}}(\tilde{F}^k, X(r_i^k) = b_i^k | X(l_i^k) = a_i^k, b_i^k \in \mathcal{E})} \\ &= \frac{\tilde{\mathbb{P}}(\tilde{F}^k, X(r_i^k) = b_i^k | X(\tau_k-) = g, b_i^k \in \mathcal{E}) \cdot \tilde{\mathbb{P}}(X(\tau_k-) = g | X(l_i^k) = a_i^k)}{\tilde{\mathbb{P}}(\tilde{F}^k, X(r_i^k) = b_i^k | X(l_i^k) = a_i^k, b_i^k \in \mathcal{E})} \\ &= \frac{\tilde{\mathbb{P}}(X(r_i^k) = b_i^k | X(\tau_k-) = g, b_i^k \in \mathcal{E}) \cdot \tilde{\mathbb{P}}(X(\tau_k-) = g | X(l_i^k) = a_i^k)}{\tilde{\mathbb{P}}(X(r_i^k) = b_i^k | X(l_i^k) = a_i^k, b_i^k \in \mathcal{E})}. \end{aligned}$$

As  $b_i^k \in \mathcal{E}$ , the subject must have been in  $\mathcal{R}_{b_i^k}$  at time  $r_i^k$ . We therefore define  $k_{r_i}$  such that  $\tau_{k_{r_i}} = r_i^k$  and condition on time  $\tau_{k_{r_i}-1}$  using the law of total probability in the numerator above:

$$\begin{aligned} \tilde{\mathbb{P}}(X(r_i^k) = b_i^k | X(\tau_k-) = g, b_i^k \in \mathcal{E}) &= \sum_{m \in \mathcal{R}_{b_i^k}} \tilde{\mathbb{P}}(X(r_i^k) = b_i^k | X(\tau_k-) = g, X(r_i^k-) = m, b_i^k \in \mathcal{E}) \cdot \\ &\quad \tilde{\mathbb{P}}(X(r_i^k-) = m | X(\tau_k-) = g, b_i^k \in \mathcal{E}) \\ &= \sum_{m \in \mathcal{R}_{b_i^k}} \tilde{\mathbb{P}}(X(r_i^k) = b_i^k | X(r_i^k-) = m, b_i^k \in \mathcal{E}) \cdot \\ &\quad \tilde{\mathbb{P}}(X(r_i^k-) = m | X(\tau_k-) = g) \\ &= \sum_{m \in \mathcal{R}_{b_i^k}} \tilde{P}_{mb_i^k}(r_i^k-, r_i^k) \tilde{P}_{gm}(\tau_{k-1}, r_i^k-) \\ &= \sum_{m \in \mathcal{R}_{b_i^k}} \tilde{\alpha}_{mb_i^k}^{k_{r_i}} \tilde{P}_{gm}(\tau_{k-1}, \tau_{k_{r_i}-1}). \end{aligned}$$

Similarly, we obtain for the denominator:

$$\tilde{\mathbb{P}}(X(r_i^k) = b_i^k | X(l_i^k) = a_i^k, b_i^k \in \mathcal{E}) = \sum_{m \in \mathcal{R}_{b_i^k}} \tilde{\alpha}_{mb_i^k}^{k r_i} \tilde{P}_{a_i^k m}(l_i^k, \tau_{k r_i - 1}).$$

Substituting these back into the original expression we obtain:

$$Y_{g,i}^k(\tilde{\alpha}) = \frac{\tilde{P}_{a_i^k g}(l_i^k, \tau_{k-1}) \cdot \sum_{m \in \mathcal{R}_{b_i^k}} \tilde{\alpha}_{mb_i^k}^{k r_i} \tilde{P}_{gm}(\tau_{k-1}, \tau_{k r_i - 1})}{\sum_{m \in \mathcal{R}_{b_i^k}} \tilde{\alpha}_{mb_i^k}^{k r_i} \tilde{P}_{a_i^k m}(l_i^k, \tau_{k r_i - 1})}. \quad (12)$$

We continue on to:

$$\begin{aligned} d_{gh,i}^k(\tilde{\alpha}) &= \tilde{\mathbb{P}}(X(\tau_k -) = g, X(\tau_k) = h | \mathbb{X}_i) \\ &= \tilde{\mathbb{P}}(X(\tau_k -) = g | \mathbb{X}_i) \cdot \tilde{\mathbb{P}}(X(\tau_k) = h | X(\tau_k -) = g, \mathbb{X}_i) \end{aligned}$$

and again focus only on the second term:

$$\begin{aligned} \tilde{\mathbb{P}}(X(\tau_k) = h | X(\tau_k -) = g, \mathbb{X}_i) &= \frac{\tilde{\mathbb{P}}(F^k | X(\tau_k) = h, b_i^k \in \mathcal{E}) \cdot \tilde{\mathbb{P}}(X(\tau_k) = h | X(\tau_k -) = g, b_i^k \in \mathcal{E})}{\tilde{\mathbb{P}}(F^k | X(\tau_k -) = g, b_i^k \in \mathcal{E})} \\ &= \frac{\tilde{\mathbb{P}}(X(r_i^k) = b_i^k | X(\tau_k) = h, b_i^k \in \mathcal{E}) \cdot \tilde{\alpha}_{gh}^k}{\tilde{\mathbb{P}}(X(r_i^k) = b_i^k | X(\tau_k -) = g, b_i^k \in \mathcal{E})}. \end{aligned}$$

The term in the denominator was already expanded above, so we focus on the term in the numerator (in a similar way as before):

$$\tilde{\mathbb{P}}(X(r_i^k) = b_i^k | X(\tau_k) = h, b_i^k \in \mathcal{E}) = \sum_{m \in \mathcal{R}_{b_i^k}} \tilde{\alpha}_{mb_i^k}^{k r_i} \tilde{P}_{hm}(\tau_k, \tau_{k r_i - 1}).$$

Substituting these results into the original expression we obtain:

$$d_{gh,i}^k = \frac{\tilde{P}_{a_i^k g}(l_i^k, \tau_{k-1}) \cdot \tilde{\alpha}_{gh}^k \cdot \sum_{m \in \mathcal{R}_{b_i^k}} \tilde{\alpha}_{mb_i^k}^{k r_i} \tilde{P}_{hm}(\tau_k, \tau_{k r_i - 1})}{\sum_{m \in \mathcal{R}_{b_i^k}} \tilde{\alpha}_{mb_i^k}^{k r_i} \tilde{P}_{a_i^k m}(l_i^k, \tau_{k r_i - 1})}. \quad (13)$$

□

## C Latent Poisson Expectation Maximisation algorithm

In this section, we loosely describe the EM algorithm for the NPMLE of panel data based on latent Poisson variables [?]. This Section therefore does not contain any original work.

Their EM algorithm is very similar to the one described in Section B, so most of the previous notation carries over. We do however need to introduce some new notation first, mainly for the latent Poisson variables. We consider the panel data observed-data likelihood. Similar to above, the cumulative intensity function is assumed to be a right-continuous step function with jumps only at the unique observation times.

Fix  $i$  and  $j$ , then  $[t_{ij-1}, t_{ij}]$  is some observation interval with observed states  $x_{ij-1}$  and  $x_{ij}$ . Let  $w$  be the value such that  $\tau_{w-1} = t_{ij-1}$ , and  $q$  the value such that  $\tau_{w+q+1} = t_{ij}$ . Then  $t_{ij-1} = \tau_{w-1} < \tau_w < \dots < \tau_{w+q} < \tau_{w+q+1} = t_{ij}$  is a grid spanning the observation interval. A transition from  $x_{ij-1}$  to  $x_{ij}$  in the observation interval must have happened through one of the possible transition paths  $(u_{w-1}, u_w, \dots, u_{w+q}, u_{w+q+1})$  with  $u_w, \dots, u_{w+q}$  the unobserved states at the corresponding times  $\tau_w, \dots, \tau_{w+q}$ . For such a possible transition path, they define the event  $V_i(u_w, \dots, u_{w+q}, t_{ij-1}, t_{ij}, x_{ij-1}, x_{ij})$  through latent Poisson random variables  $W_{gh,i}^k$  as follows. For  $k = w, \dots, w+q+1$ , if  $u_{k-1} \neq u_k$  then  $W_{u_{k-1}u_k,i}^k > 0$  and  $W_{u_{k-1}u',i}^k = 0$  for all  $u' \neq u_{k-1}, u_k$ . Else if  $u_{k-1} = u_k$  we have that  $W_{u_{k-1}u',i}^k = 0$  for all  $u' \neq u_{k-1}$ . They then define the event  $Y_i(t_{ij-1}, t_{ij}, x_{ij-1}, x_{ij}) = \bigcup_{(u_w, \dots, u_{w+q}) \in \mathcal{A}_{w+q}} V_i(u_w, \dots, u_{w+q}, t_{ij-1}, t_{ij}, x_{ij-1}, x_{ij})$  with  $\mathcal{A}_{w+q}$  the set of possible transitions connecting  $x_{ij-1}$  and  $x_{ij}$ . They show that maximising the panel data observed-data likelihood is the same as maximising the likelihood based on the observations  $\mathcal{O}_i = \bigcap_{j=1}^{r_i} Y_i(t_{ij-1}, t_{ij}, x_{ij-1}, x_{ij})$ .

They show that the complete-data log likelihood for these latent Poisson variables is given by:

$$\ell^P = \sum_{i=1}^n \left( \sum_{k=1}^K \sum_{(g,h) \in \mathcal{V}} \mathbb{1}\{\tau_k \leq t_{in_i}\} [W_{gh,i}^k \log(\alpha_{gh}^k) - \alpha_{gh}^k - \log(W_{gh,i}^k!)] \right) \quad (14)$$

This likelihood is quite different compared to the complete-data log likelihood based on the multinomial distribution considered by us.

To determine an update rule for  $\alpha_{gh}^k$ , they calculate the conditional expectation of the Poisson variables given the observed data and current estimates of the transition intensities:

$$\tilde{\mathbb{E}}[W_{gh,i}^k | O] = \mathbb{E}[W_{gh,i}^k | O, \tilde{\alpha}] = \frac{\sum_{g' \neq g} \tilde{P}_{a_i^k g'}(l_i^k, \tau_k -) \tilde{P}_{g' b_i^k}(\tau_k -, r_i^k)}{\tilde{P}_{a_i^k b_i^k}(l_i^k, r_i^k)} \tilde{\alpha}_{gh}^k \quad (15)$$

$$+ \frac{\tilde{P}_{a_i^k g}(l_i^k, \tau_k -) \tilde{\alpha}_{gh}^k \tilde{P}_{h b_i^k}(\tau_k, r_i^k)}{\tilde{P}_{a_i^k b_i^k}(l_i^k, r_i^k)} \exp \left( - \sum_{h' \leftarrow g, h' \neq h} \tilde{\alpha}_{gh'}^k \right) \quad (16)$$

The update rule (M-step) in the EM algorithm is then given by:

$$\alpha_{gh}^k = \frac{\sum_{i=1}^n \mathbb{1}\{\tau_k \leq t_{i,n_i}\} \tilde{\mathbb{E}}[W_{gh,i}^k | O]}{\sum_{i=1}^n \mathbb{1}\{\tau_k \leq t_{i,n_i}\}} \quad (17)$$

Contrary to our approach in Section B they do not consider the KKT conditions to make sure that (sum of the) updated intensities is bounded by zero and one in the M-step. In practice, this is unlikely to be an issue in non-parametric estimation, but might be problematic when covariates are included.

## D Latent Poisson EM - initial estimate dependence

In this section, we show that the initial intensity estimates for transitions out of non-absorbing states that are not covered by the initial state cannot be changed by the latent Poisson approach.

Consider  $g, h \in \mathcal{H}$  such that the transition  $g \rightarrow h$  is possible. Assume that no subject starts at time 0 in state  $g$ . Consider the first bin  $[0, \tau_1]$  and a single subject  $i \in \{1, \dots, n\}$ . The contribution of this subject to the value of  $\alpha_{gh}^1$  is given by Equation (15):

$$\begin{aligned} \tilde{E}[W_{gh,i}^1 | O] &= \frac{\sum_{g' \neq g} \tilde{P}_{a_i^1 g'}(l_i^1, \tau_1 -) \tilde{P}_{g' b_i^1}(\tau_1 -, r_i^1)}{\tilde{P}_{a_i^1 b_i^1}(l_i^1, r_i^1)} \tilde{\alpha}_{gh}^1 \\ &+ \frac{\tilde{P}_{a_i^1 g}(l_i^1, \tau_1 -) \tilde{\alpha}_{gh}^1 \tilde{P}_{h b_i^1}(\tau_1, r_i^1)}{\tilde{P}_{a_i^1 b_i^1}(l_i^1, r_i^1)} \exp \left( - \sum_{h' \leftarrow g, h' \neq h} \tilde{\alpha}_{gh'}^1 \right) \end{aligned}$$

Clearly  $l_i^1 = \tau_1 - = 0$ , so we obtain:

$$\begin{aligned} \tilde{E}[W_{gh,i}^1 | O] &= \frac{\sum_{g' \neq g} \tilde{P}_{a_i^1 g'}(0, 0) \tilde{P}_{g' b_i^1}(0, r_i^1)}{\tilde{P}_{a_i^1 b_i^1}(0, r_i^1)} \tilde{\alpha}_{gh}^1 \\ &+ \frac{\tilde{P}_{a_i^1 g}(0, 0) \tilde{\alpha}_{gh}^1 \tilde{P}_{h b_i^1}(\tau_1, r_i^1)}{\tilde{P}_{a_i^1 b_i^1}(0, r_i^1)} \exp \left( - \sum_{h' \leftarrow g, h' \neq h} \tilde{\alpha}_{gh'}^1 \right) \end{aligned}$$

Note that  $\tilde{P}_{a_i^1 g'}(0, 0)$  can only be non-zero when  $g' = a_i^1$ . The summation in the numerator of the first term therefore only yields a positive contribution when  $g' = a_i^1$ . As we assumed that no subjects start in state  $g$ , we must have that  $g \neq a_i^1$  and therefore the second term is 0. We obtain:

$$\tilde{E}[W_{gh,i}^1 | O] = \frac{\sum_{g' \neq g} \tilde{P}_{a_i^1 g'}(0, 0) \tilde{P}_{g' b_i^1}(0, r_i^1)}{\tilde{P}_{a_i^1 b_i^1}(0, r_i^1)} \tilde{\alpha}_{gh}^1 = \frac{\tilde{P}_{a_i^1 a_i^1}(0, 0) \tilde{P}_{a_i^1 b_i^1}(0, r_i^1)}{\tilde{P}_{a_i^1 b_i^1}(0, r_i^1)} \tilde{\alpha}_{gh}^1 = \tilde{\alpha}_{gh}^1$$

Therefore the contribution of all subjects is the same at each iteration. From Equation (17) we then find that the estimate of  $\tilde{\alpha}_{gh}^1$  does not change over any iteration and the final estimate will simply be the initial estimate. The result shown here can also be extended to any  $W_{gh,i}^k$  where no subject can be in state  $g$  before time  $\tau_k$ . The summation in the numerator of the first term of Equation (15) represents the probability of reaching  $b_i^k$  through any path that does not go through state  $g$  at time  $\tau_k-$ . The denominator represents the probability of reaching  $b_i^k$  through any path. As we assume that no subject can be in state  $g$  at time  $\tau_k-$ , the numerator and denominator are equal and therefore the first term simply becomes  $\tilde{\alpha}_{gh}^k$ . The second term represents the probability of making the  $g \rightarrow h$  transition in the bin  $(\tau_k-, \tau_k]$ , but as we assumed no subject can be in state  $g$  at time  $\tau_k-$  this probability clearly is zero. This means that the estimate for the transition intensities cannot be changed for an interval where there is zero probability to be in state  $g$  at the start of that interval.

## E Simulation Study - Figures

This section presents the complete results concerning performance measures in the four considered scenarios.

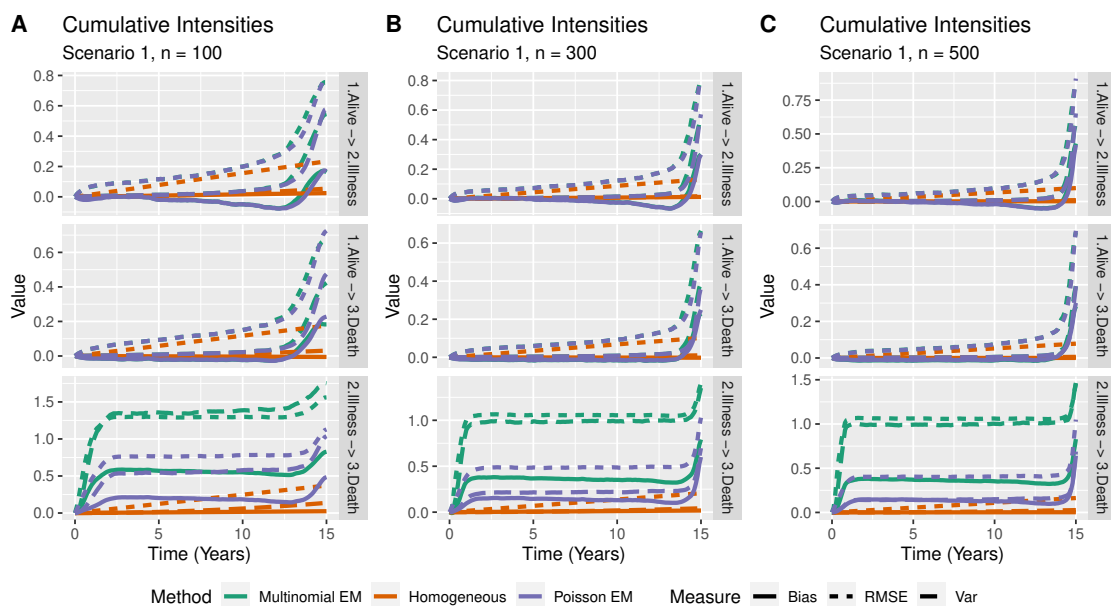


Figure 2: Bias, Variance and RMSE of cumulative intensities in scenario 1 for A)  $n = 100$ , B)  $n = 300$ , C)  $n = 500$  samples in  $N = 1000$  simulated data sets.



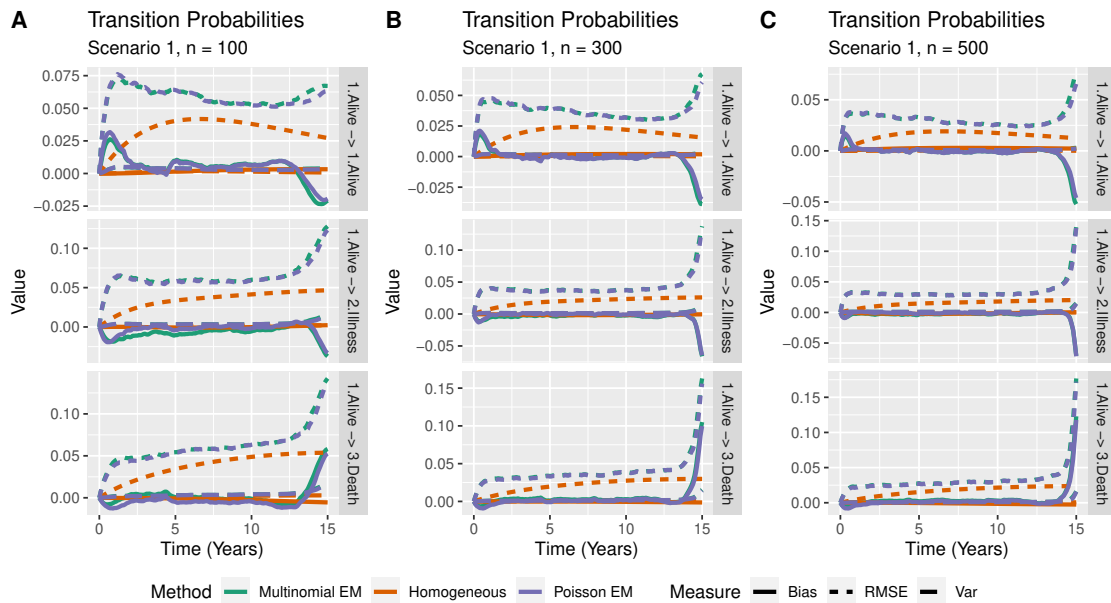


Figure 3: Bias, Variance and RMSE of transition probabilities in scenario 1 for A)  $n = 100$ , B)  $n = 300$ , C)  $n = 500$  samples in  $N = 1000$  simulated data sets.

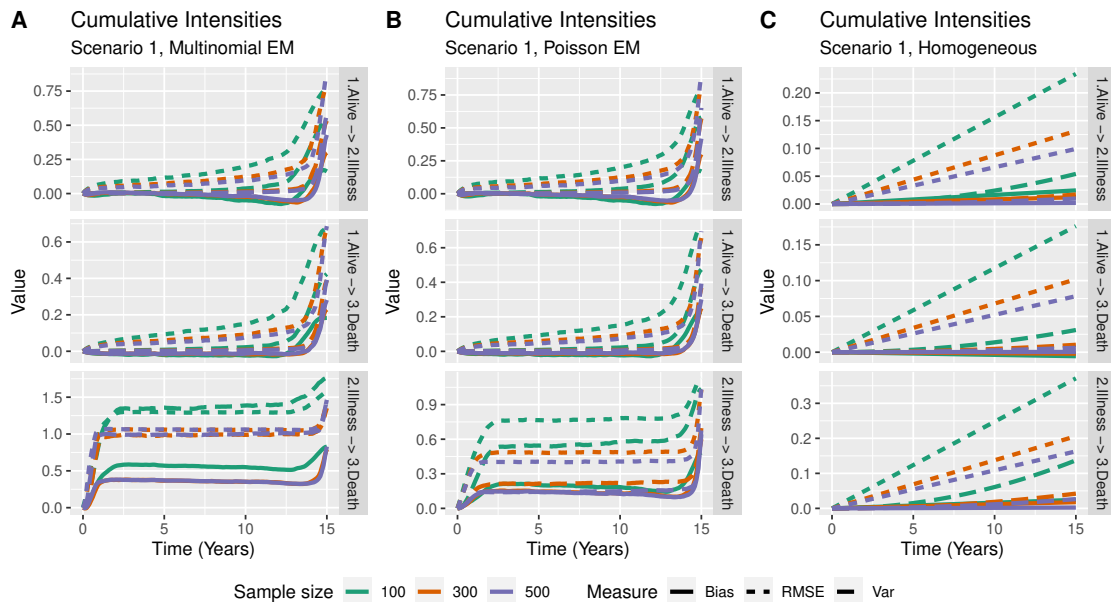


Figure 4: Bias, Variance and RMSE of cumulative intensities in scenario 1 for A) Binomial EM, B) Poisson EM, C) Time-homogeneous methods in  $N = 1000$  simulated data sets.

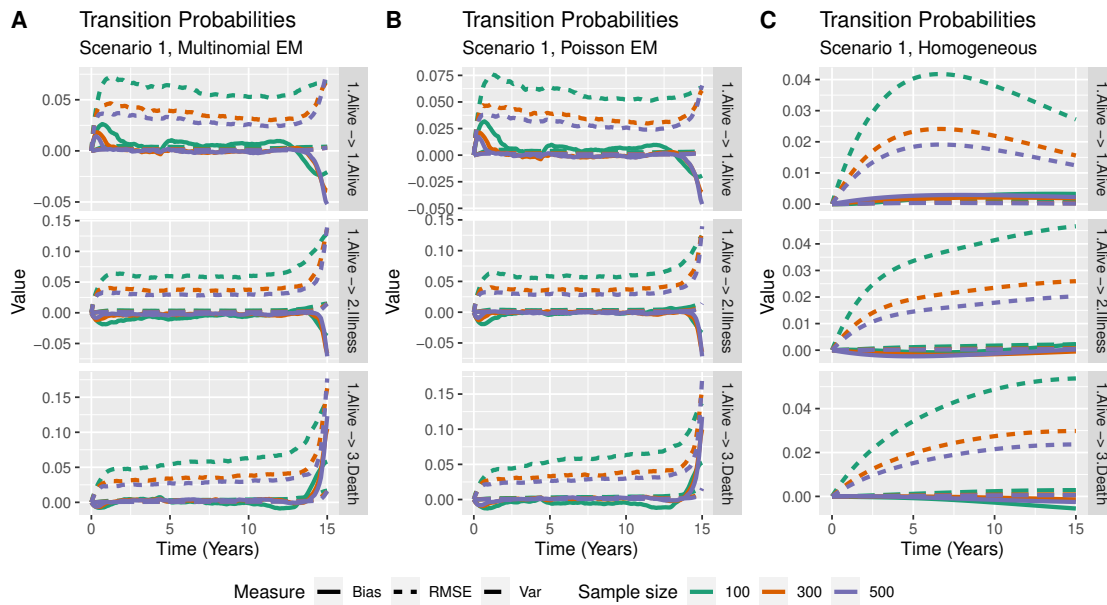


Figure 5: Bias, Variance and RMSE of transition probabilities in scenario 1 for A) Binomial EM, B) Poisson EM, C) Time-homogeneous methods in  $N = 1000$  simulated data sets.

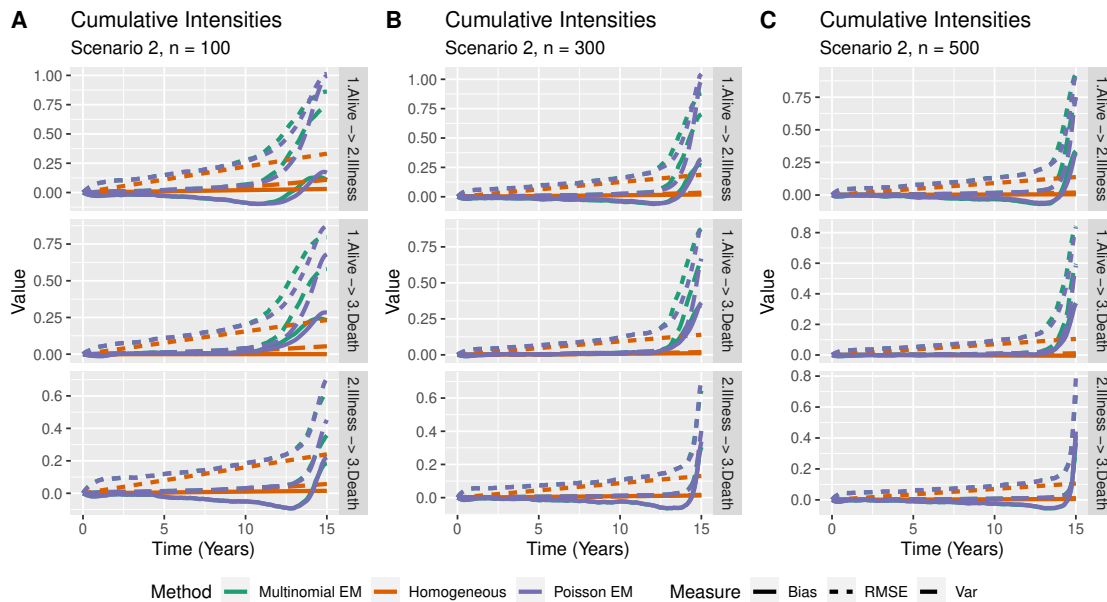


Figure 6: Bias, Variance and RMSE of cumulative intensities in scenario 2 for A)  $n = 100$ , B)  $n = 300$ , C)  $n = 500$  samples in  $N = 1000$  simulated data sets.

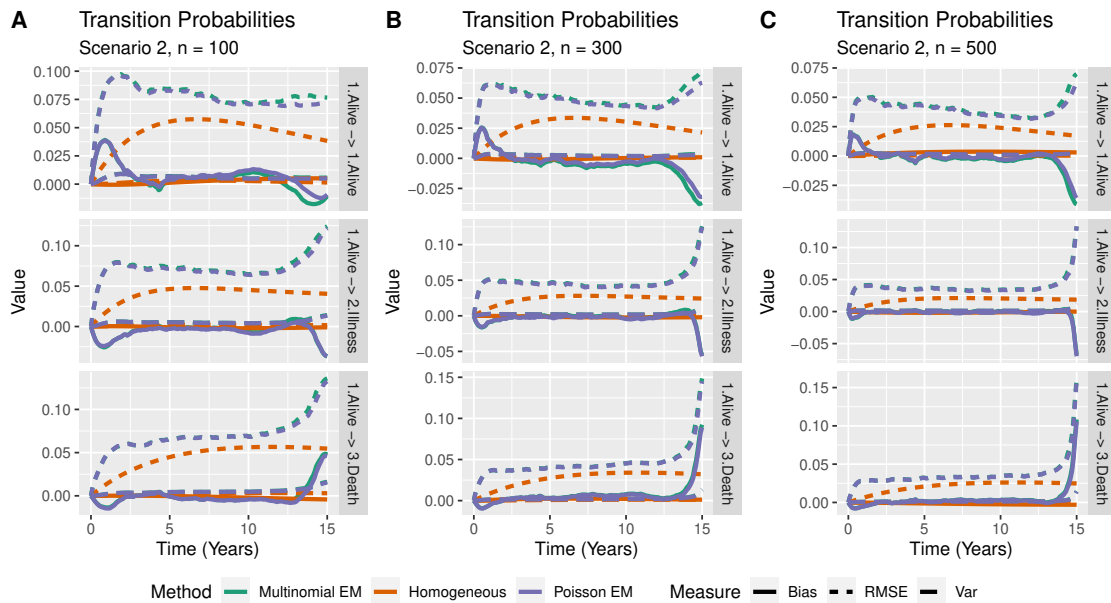


Figure 7: Bias, Variance and RMSE of transition probabilities in scenario 2 for A)  $n = 100$ , B)  $n = 300$ , C)  $n = 500$  samples in  $N = 1000$  simulated data sets.

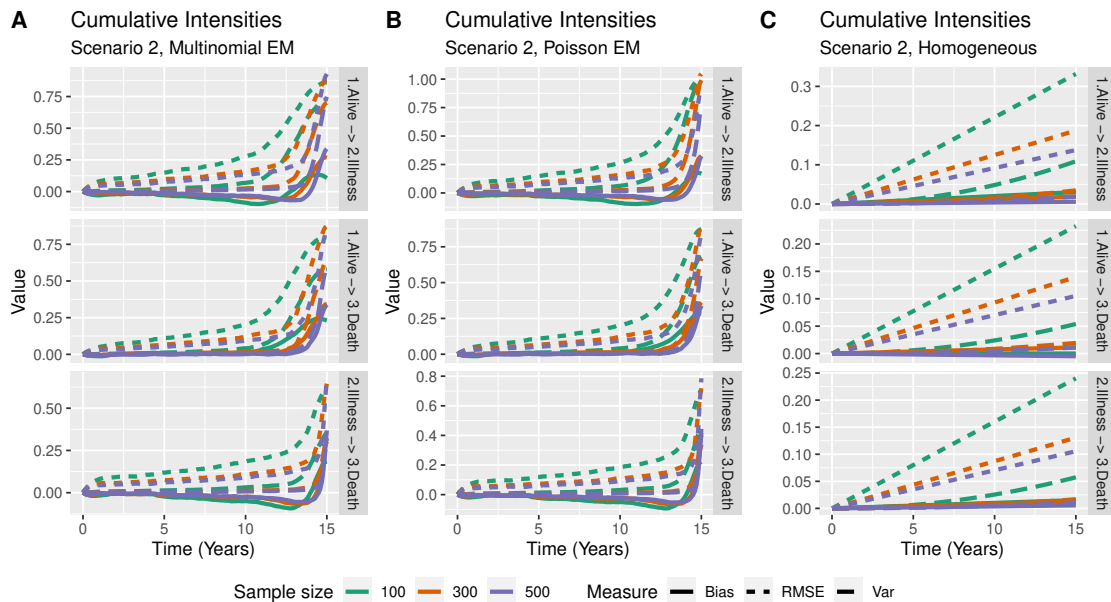


Figure 8: Bias, Variance and RMSE of cumulative intensities in scenario 2 for A) Binomial EM, B) Poisson EM, C) Time-homogeneous methods in  $N = 1000$  simulated data sets.

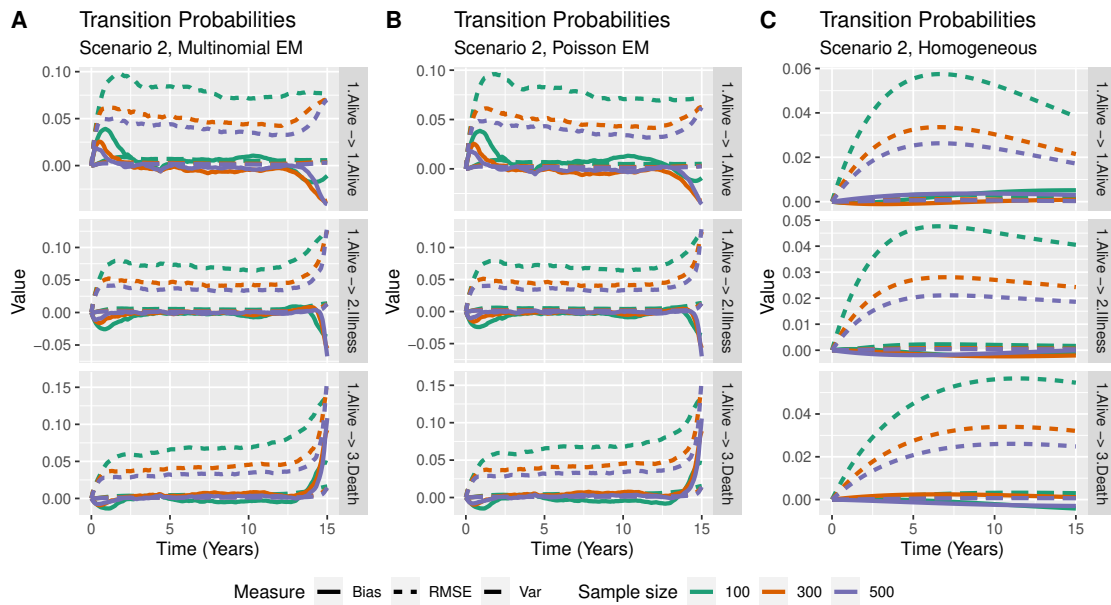


Figure 9: Bias, Variance and RMSE of transition probabilities in scenario 2 for A) Binomial EM, B) Poisson EM, C) Time-homogeneous methods in  $N = 1000$  simulated data sets.

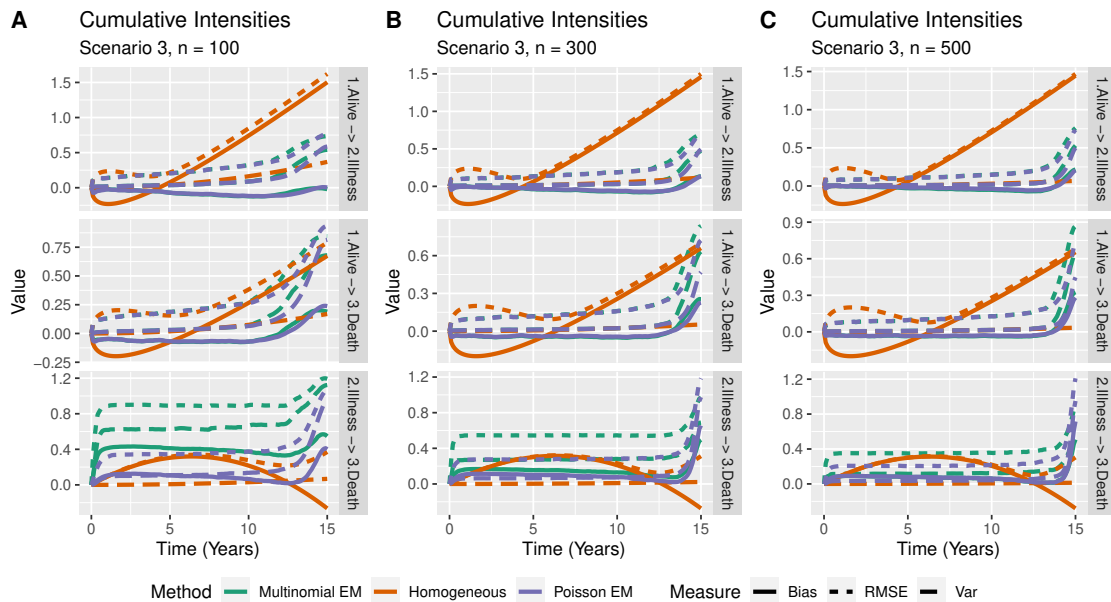


Figure 10: Bias, Variance and RMSE of cumulative intensities in scenario 3 for A)  $n = 100$ , B)  $n = 300$ , C)  $n = 500$  samples in  $N = 1000$  simulated data sets.

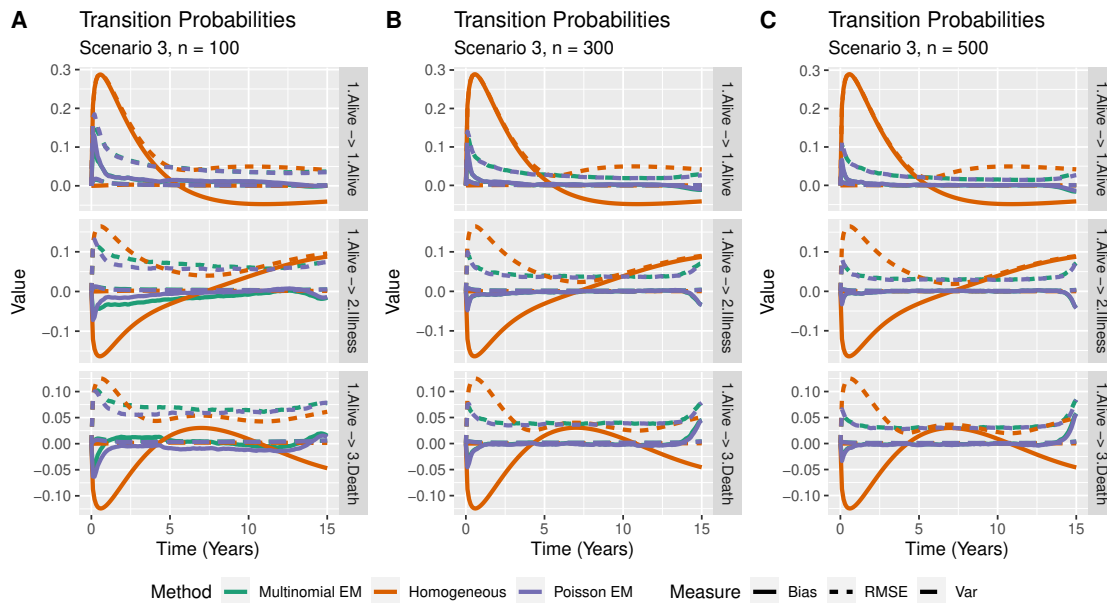


Figure 11: Bias, Variance and RMSE of transition probabilities in scenario 3 for A)  $n = 100$ , B)  $n = 300$ , C)  $n = 500$  samples in  $N = 1000$  simulated data sets.

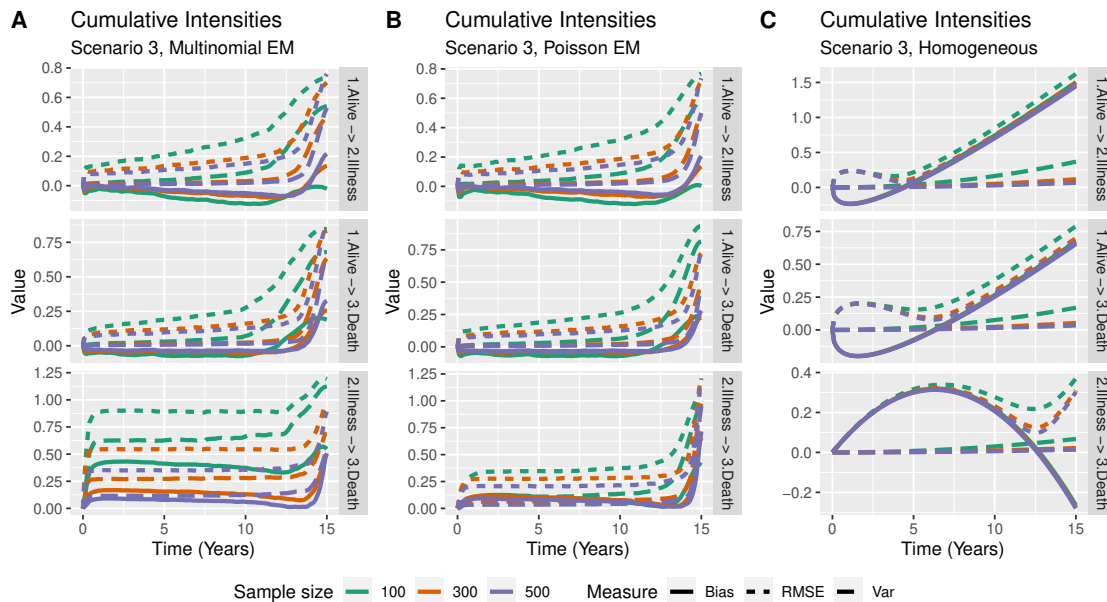


Figure 12: Bias, Variance and RMSE of cumulative intensities in scenario 3 for A) Binomial EM, B) Poisson EM, C) Time-homogeneous methods in  $N = 1000$  simulated data sets.

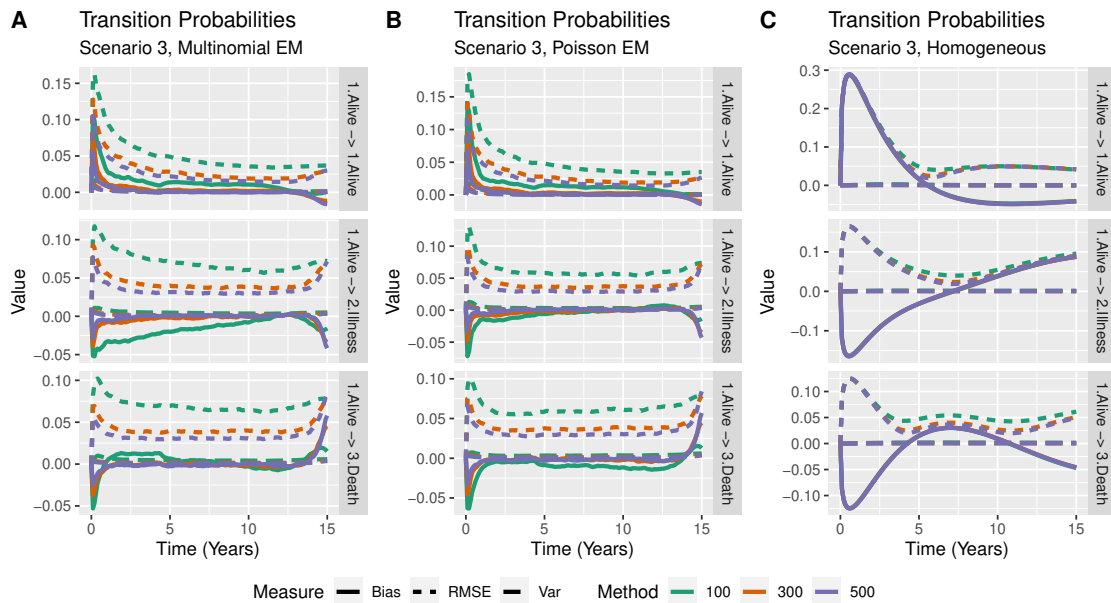


Figure 13: Bias, Variance and RMSE of transition probabilities in scenario 3 for A) Binomial EM, B) Poisson EM, C) Time-homogeneous methods in  $N = 1000$  simulated data sets.

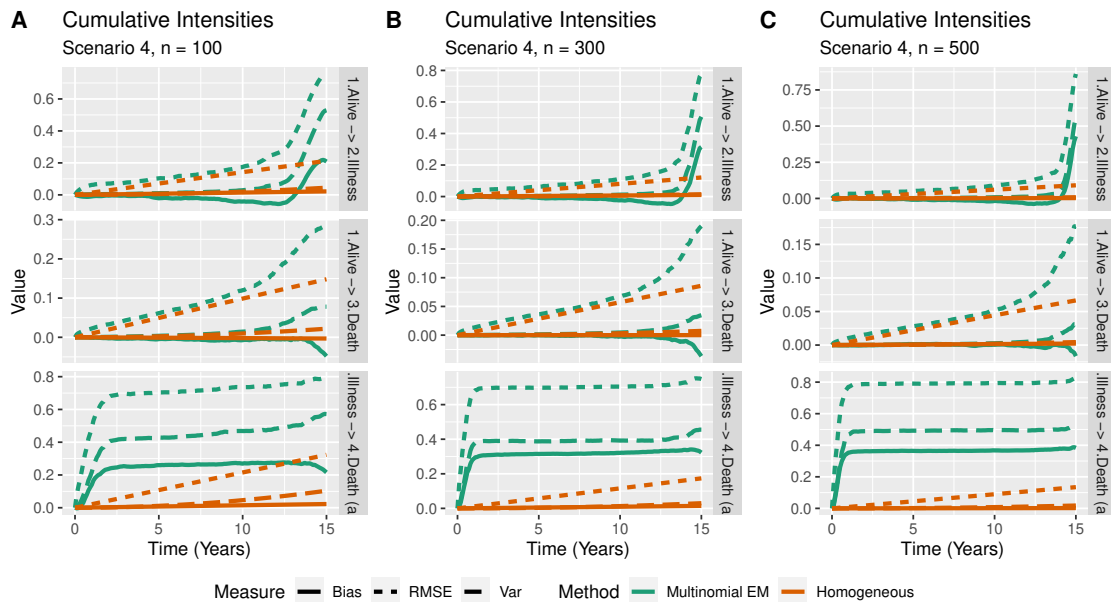


Figure 14: Bias, Variance and RMSE of cumulative intensities in scenario 4 for A)  $n = 100$ , B)  $n = 300$ , C)  $n = 500$  samples in  $N = 1000$  simulated data sets.

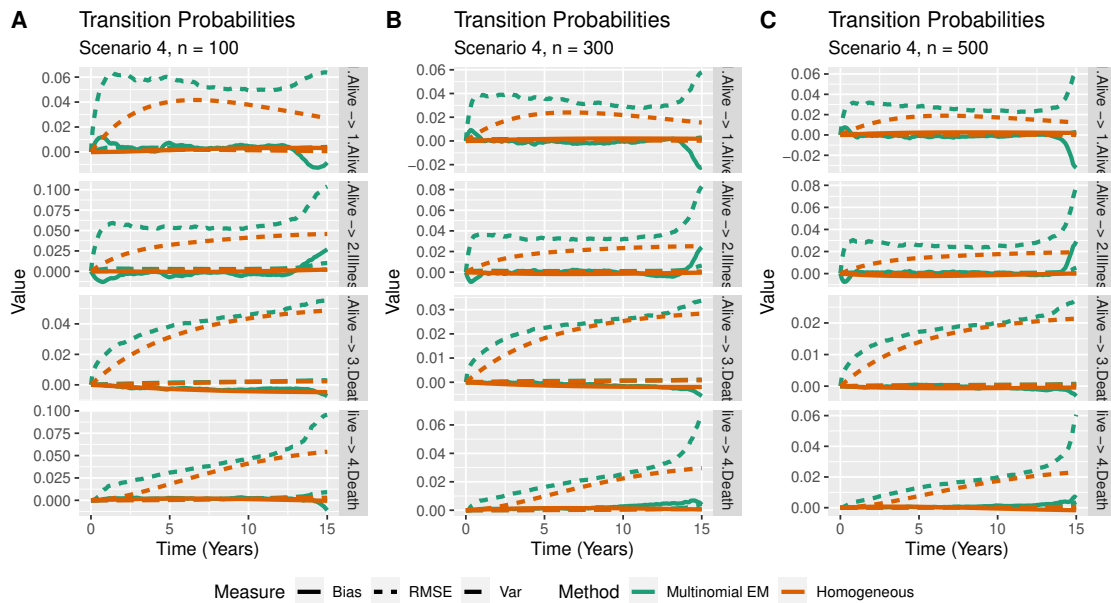


Figure 15: Bias, Variance and RMSE of transition probabilities in scenario 4 for A)  $n = 100$ , B)  $n = 300$ , C)  $n = 500$  samples in  $N = 1000$  simulated data sets.

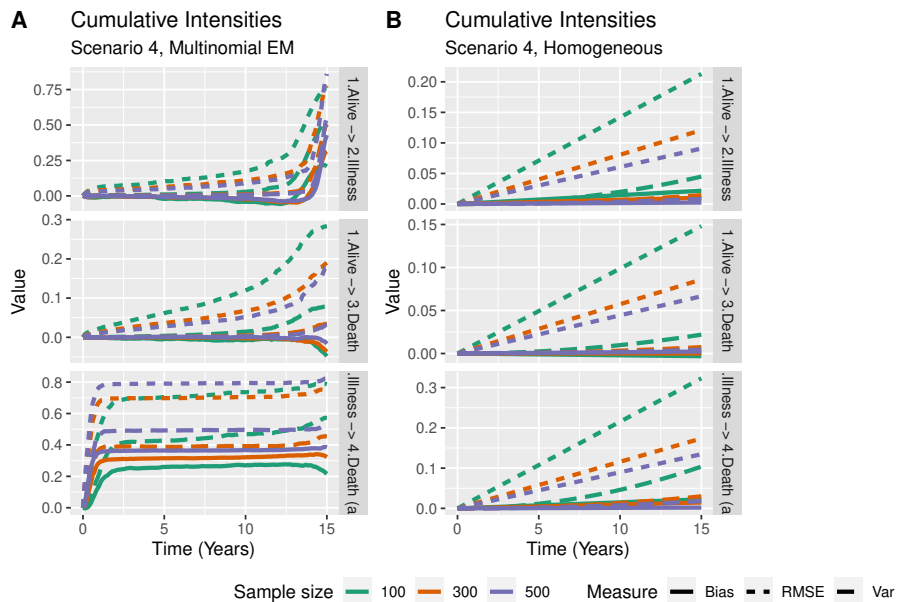


Figure 16: Bias, Variance and RMSE of cumulative intensities in scenario 4 for A) Binomial EM, B) Time-homogeneous methods in  $N = 1000$  simulated data sets.

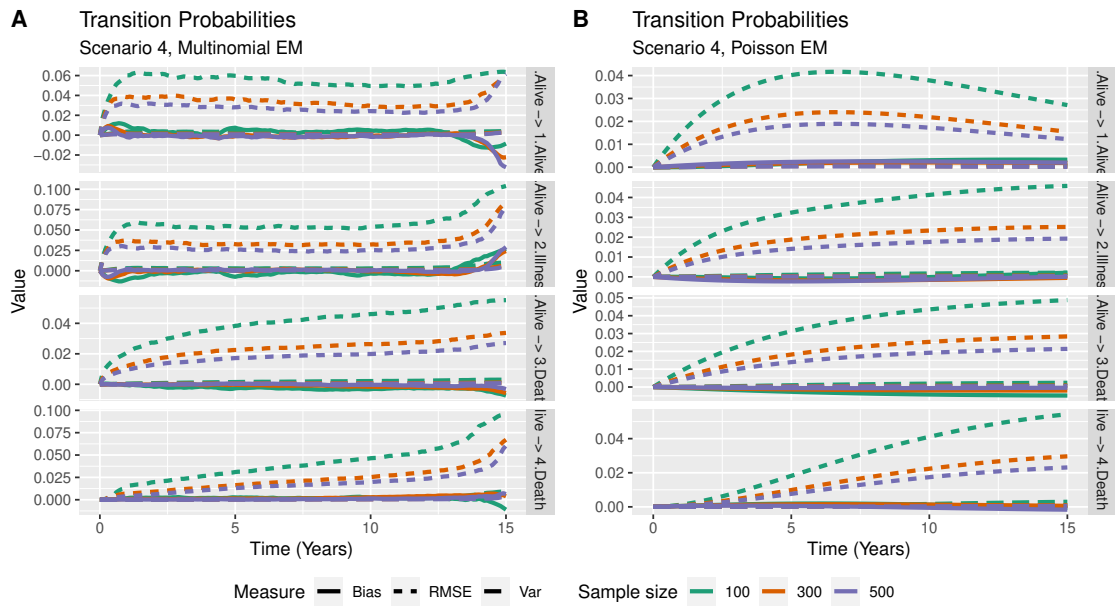


Figure 17: Bias, Variance and RMSE of transition probabilities in scenario 4 for A) Binomial EM, B) Poisson EM, C) Time-homogeneous methods in  $N = 1000$  simulated data sets.